STRUCTURAL CHEMISTRY

ISSN 2053-2296

Role of secondary interactions in a series of 2:1 halogen-bonded cocrystals formed between 4-(dimethylamino)pyridine and ditopic halogen-bond donors

Eric Bosch[a]* and Nathan P. Bowling[b]

[a]Chemistry and Biochemistry Department, Missouri State University, 901 South National Avenue, Springfield, MO 65897, USA, and [b]Department of Chemistry, University of Wisconsin-Stevens Point, 2101 Fourth Avenue, Stevens Point, WI 54481, USA. *Correspondence e-mail: ericbosch@missouristate.edu

Received 11 June 2024
Accepted 5 August 2024

Edited by I. Oswald, University of Strathclyde, United Kingdom

Keywords: crystal structure; halogen bonding; 1,4-diiodotetrahalobenzene; C—Cl···π; C—Br···π; C—H···π.

CCDC references: 2375541; 2375540; 2375539; 2375538

Supporting information: this article has supporting information at journals.iucr.org/c

The structures of a series of 2:1 cocrystals formed between 4-(dimethylamino)pyridine and each of 1,2,4,5-tetrachloro-3,6-diiodobenzene, $2C_7H_{10}N_2{\cdot}C_6Cl_4I_2$, 1,2,4,5-tetrabromo-3,6-diiodobenzene, $2C_7H_{10}N_2{\cdot}C_6Br_4I_2$, 1-bromo-4-iodo-2,3,5,6-tetrafluorobenzene, $2C_7H_{10}N_2{\cdot}C_6BrF_4I$, and 1,2-dibromo-4,5-difluoro-3,6-diiodobenzene, $2C_7H_{10}N_2{\cdot}C_6Br_2F_2I_2$, are reported. In all five structures, the core halogen-bonded 2:1 trimolecular units have geometrically similar parameters, with the central halogen-bond donor flanked by two pyridine halogen-bond acceptors twisted with respect to the central halogen-bond donor at angles ranging from 76 to 86°. The I···N halogen-bond separations are all short, ranging from 73.3 to 76.7% of the sum of the van der Waals radii, while the C—I···N bond angles are essentially linear. The Br···N halogen-bond separation in the cocrystal formed with 1-bromo-4-iodo-2,3,5,6-tetrafluorobenzene is 80.4% of the sum of the van der Waals radii. Subtle differences in the crystal packings are attributed to the role of secondary C—H···π and weak π-type interactions with chloro and bromo substituents. The cocrystals $2C_7H_{10}N_2{\cdot}C_6Cl_4I_2$ and $2C_7H_{10}N_2{\cdot}C_6Br_4I_2$ are isomorphous.

1. Introduction

The halogen bond is a net attractive interaction between the electrophilic region on a bonded halogen atom, called a σ-hole, with a nucleophilic region on another molecular entity, often a nonbonding electron pair or a π-system (Desiraju *et al.*, 2013). This is now a mature field of study with potential applications in a wide variety of fields, including liquid crystals, anion sensing, porous materials, and solid-state synthesis (Cavallo *et al.*, 2016; Gilday *et al.*, 2015; Costa, 2017). Vital to the development of the field were experimental and computational studies that revealed the theory and principles that now allow the deliberate synthesis of components for desired supramolecular assemblies. Thus, it is now understood that the intensity of the electrophilic region on the halogen-bond donor decreases in the order I > Br > Cl and further that the positive electrostatic potential, the σ-hole, is amplified by proximal electron-withdrawing groups (Politzer *et al.*, 2010). While fluorine substitution is most common, other electron-withdrawing groups in the organic chemist's toolbox have been shown to have a dramatic effect on the intensity of the σ-hole. For example, it has been shown that a proximal nitro group leads to exceptionally strong halogen-bond donors (Bennion *et al.*, 2016), as well as combinations of proximal electron-withdrawing groups (Panikkattu *et al.*, 2022). One of the early studies that investigated the influence of proximal F

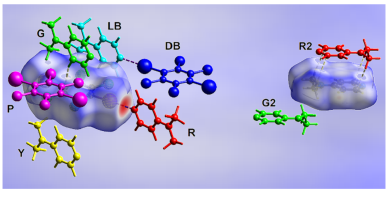

Table 1
Experimental details.

Experiments were carried out at 100 K with Cu $K\alpha$ radiation using a Rigaku XtaLAB Synergy Dualflex diffractometer with a HyPix detector. The absorption correction was analytical (*CrysAlis PRO*; Rigaku OD, 2023) using a multifaceted crystal model based on expressions derived by Clark & Reid (1995). H-atom parameters were constrained.

	2DMAP·DITCB	**2DMAP·DITBB**	**2DMAP·IBTFB**	**2DMAP·DIBFB**
Crystal data				
Chemical formula	$2C_7H_{10}N_2{\cdot}C_6Cl_4I_2$	$2C_7H_{10}N_2{\cdot}C_6Br_4I_2$	$2C_7H_{10}N_2{\cdot}C_6BrF_4I$	$2C_7H_{10}N_2{\cdot}C_6Br_2F_2I_2$
M_r	712.03	889.83	599.21	768.02
Crystal system, space group	Triclinic, $P\overline{1}$	Triclinic, $P\overline{1}$	Monoclinic, $P2_1/c$	Triclinic, $P\overline{1}$
a, b, c (Å)	8.1680 (3), 9.1290 (4), 9.8118 (3)	8.3361 (2), 9.3089 (3), 9.8204 (2)	7.3898 (1), 16.2120 (2), 9.4236 (1)	9.6158 (4), 9.7518 (4), 14.8423 (7)
α, β, γ (°)	103.727 (3), 107.165 (3), 112.180 (4)	102.484 (2), 108.399 (2), 113.064 (2)	90, 106.304 (2), 90	74.473 (4), 85.820 (4), 61.476 (4)
V (Å^3)	594.91 (5)	612.84 (4)	1083.58 (3)	1175.73 (10)
Z	1	1	2	2
μ (mm^{-1})	25.03	27.92	14.21	25.26
Crystal size (mm)	0.14 × 0.1 × 0.03	0.21 × 0.17 × 0.08	0.12 × 0.08 × 0.05	0.23 × 0.1 × 0.04
Data collection				
T_{min}, T_{max}	0.104, 0.510	0.011, 0.146	0.357, 0.595	0.055, 0.441
No. of measured, independent and observed [$I \geq 2\sigma(I)$] reflections	8921, 2500, 2413	11315, 2446, 2429	10454, 2300, 2252	22021, 4962, 4694
R_{int}	0.063	0.055	0.042	0.063
$(\sin\theta/\lambda)_{max}$ (Å^{-1})	0.634	0.632	0.634	0.635
Refinement				
$R[F^2 > 2\sigma(F^2)]$, $wR(F^2)$, S	0.038, 0.107, 1.02	0.039, 0.110, 1.03	0.034, 0.080, 1.00	0.049, 0.142, 1.03
No. of reflections	2500	2446	2300	4962
No. of parameters	138	138	142	275
No. of restraints	0	0	2	0
$\Delta\rho_{max}$, $\Delta\rho_{min}$ (e Å^{-3})	1.33, −1.51	1.81, −1.59	0.75, −0.58	3.00, −1.94

Computer programs: *CrysAlis PRO* (Rigaku OD, 2023), *SHELXT2014* (Sheldrick, 2015), *SHELXT2018* (Sheldrick, 2015), *olex2.refine* (Bourhis *et al.*, 2015), *X-Seed* (Barbour, 2020), and *OLEX2* (Dolomanov *et al.*, 2009).

atoms on the separation between the halogen-bond donor and the halogen-bond acceptor looked at the structures of a series of cocrystals formed between the halogen-bond acceptor 4-(dimethylamino)pyridine and fluorinated iodobenzenes as halogen-bond donors (Präsang *et al.*, 2009). This study established that the I···N separation was directly correlated to the number of F atoms on the iodobenzene, with the shortest distance observed for pentafluoroiodobenzene. Here, we present a similar study with a series of ditopic halogen-bond donors initially prepared as prospective halogen-bond donors for the solid-state photodimerization of alkenes (Bosch *et al.*, 2019). In particular, we present a series of substituted benzenes as linear ditopic halogen-bond donors, including 1,2,4,5-tetrachloro-3,6-diiodobenzene (**DITCB**), 1,2,4,5-tetrabromo-3,6-diiodobenzene (**DITBB**), 1,2-dibromo-4,5-difluoro-3,6-diiodobenzene (**DIFBB**), and 1,2,4,5-tetrafluoro-3-bromo-6-iodobenzene (**BITFB**). Since most of these donors are less activated than the prototypical linear ditopic halogen-bond donor 1,2,4,5-tetrafluoro-3,6-diiodobenzene (**DITFB**), we chose the same strong pyridine-based halogen-bond acceptor 4-(dimethylamino)pyridine (**DMAP**), to best ensure the isolation of a complete series of cocrystals. In each case, 2:1 cocrystals were formed and we compare these data to those previously reported for similar cocrystallization with **DITFB** (Wang *et al.*, 2018; Roper *et al.*, 2010). A search of the Cambridge Structural Database (CSD; Groom *et al.*, 2016) for cocrystals formed by pyridines, with any substitution pattern, and per-halogenated 1,4-diiodobenzenes yielded 310 structures corresponding to 212 distinct cocrystals. Amongst these are 2:1 cocrystals and 1:1 cocrystals that include 1,2-bis-(pyridyl)ethenes as halogen-bond acceptor and are photoactive (Bosch *et al.*, 2019; Quentin & MacGillivray, 2020). In a recent study, the 1:1 cocrystal formed between **DITFB** and the dipyridyl 2,5-bis(pyridin-4-yl)thiazolo[5,4-*d*]thiazole has application as an organic scintillator (Chen *et al.*, 2024).

2. Experimental

2.1. Materials

The perhalobenzene compounds **DITCB** (Reddy *et al.*, 2006), **DITBB** (Lu *et al.*, 2004), **IBTFB** (Aakeroy *et al.*, 2013), and **DIBFB** (LG Limited, 2019) used in this study have been synthesized previously. They were synthesized as reported or with known iodination procedures and gave identical spectroscopic data.

2.2. Formation of cocrystals

In each case, the pair of compounds were weighed out with a 2:1 molar ratio. Thus, 23.2 mg (0.05 mmol) of **DITCB** and 12.1 mg (0.10 mmol) of **DMAP** were added to a screw-cap vial. After chloroform (2 ml) was added, the vial was sealed, vortexed, and heated gently to ensure complete dissolution of the solids. The cap was loosened and the solvent was allowed

to evaporate slowly. After partial evaporation, a homogeneous mass of crystals formed and these were separated and dried on filter paper (27.8 mg). The other cocrystals followed this procedure giving similar yields of crystals. The cocrystal formed between **DITBB** and **DMAP** yielded a single large block-shaped crystal that was cut for analysis.

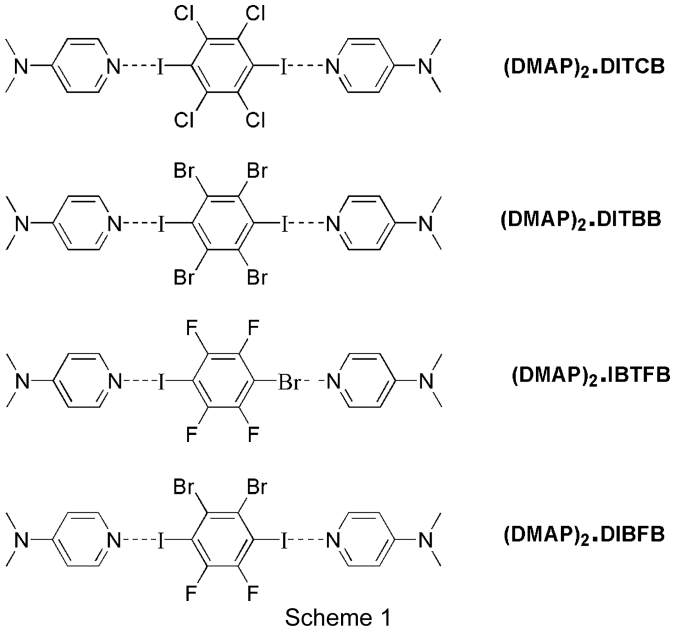

Scheme 1

2.3. Molecular electrostatic potential (MEP) calculations

The perhalobenzenes used in this study and 1,2,4,5-tetrafluoro-3,6-diiodobenzene were geometry optimized using the *SPARTAN'20* (Version 1.1.4) molecular-modeling program, with density functional theory (DFT) at the B3LYP/6-311 ++G** level (Wavefunction, 2022). The corresponding MEP energy surface was then calculated with an isovalue of 0.2 e au^{-3}.

2.4. X-ray structure determination

Crystal data, data collection and structure refinement details are summarized in Table 1. In all structures, residual electron-density corresponding to the positions of the H atoms bound to C atoms was observed in a difference Fourier map. H atoms were then added geometrically constrained using the appropriate AFIX commands. In cocrystal **(DMAP)$_2$·(IBTFB)**, the Br and I atoms are disordered between two positions and were modeled with an occupancy of 0.5 in positions 1 and 4. They were then refined with distance restraints of C—Br = 1.85 (2) Å and C—I = 2.09 (2) Å, as equivalent anisotropic displacement parameters (EADP) for Br and I. Interplanar distances were calculated using the GEOMETRY function run in *PLATON* (Spek, 2020).

2.5. Hirshfeld surface and intermolecular energy calculations

The program *CrystalExplorer21* (Spackman *et al.*, 2021) was used to calculate the Hirshfeld surface of each molecule within each structure. Fingerprint analysis of the contacts provide an element-to-element breakdown of the intermolecular contacts. The program was also used to calculate the intermolecular interaction energies between molecules within the crystal structure. The disorder of the I and Br atoms in the 1-bromo-4-iodotetrafluorobenzene cocrystal **(DMAP)$_2$·IBTFB** precludes effective Hirshfeld calculations. To provide a comparison with a tetrafluoro analogue, Hirshfeld surface calculations were performed using the published structure of

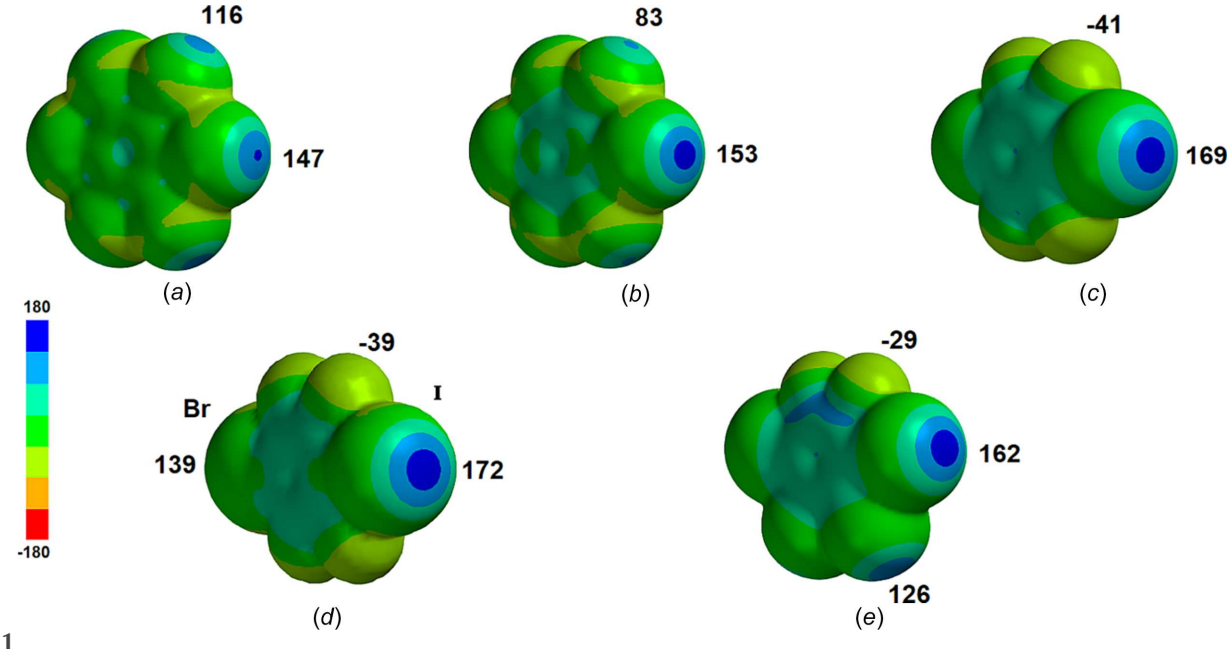

Figure 1
Plot showing the molecular electrostatic potential plot for (*a*) **DITBB**, (*b*) **DITCB**, (*c*) **DITFB**, (*d*) **IBTFB**, and, for comparison, (*e*) **DIBFB**. All plots are drawn with the same scale: −180 to 180 kJ mol^{-1}.

cocrystal **(DMAP)$_2$·DITFB** (Wang *et al.*, 2018; Roper *et al.*, 2010).

3. Results and discussion

3.1. Molecular electrostatic potential (MEP) calculations

The MEP surfaces were calculated for each of the compounds in this study and for 1,2,4,5-tetrafluoro-3,6-diiodobenzene (**DITFB**), for comparison, under the same conditions. The maxima shown in Fig. 1 highlight the dramatic decrease in the positive σ-hole on the I atom in the order $C_6F_4I_2 > C_6Cl_4I_2 > C_6Br_4I_2$, with maxima of 169, 153, and 147 kJ mol^{-1}, respectively. This is accompanied by a shift from a negative electrostatic potential on the F atoms in **DITFB** of −41 kJ mol^{-1} to secondary centres of electropositive potential on the Cl and Br atoms in **DITCB** and **DITBB** of 83 and 116 kJ mol^{-1}, respectively. The calculated maximum electrostatic potential for the σ-hole on the I atom in **IBTFB** is 172 kJ mol^{-1}, with a maximum on Br of 139 kJ mol^{-1}, while the F atoms have negative electrostatic potential of −39 kJ mol^{-1}. The compound **DIBFB** has a positive electrostatic potential on each I atom of 162 kJ mol^{-1}, and 126 kJ mol^{-1} on each Br atom, along with a negative value of −29 kJ mol^{-1} on the F atoms.

3.2. Cocrystal structures

The four 2:1 cocrystals were formed by slow evaporation of chloroform solutions containing a 2:1 molar ratio of 4-(dimethylamino)pyridine with each of the perhalobenzenes and, in each case, yielded a homogeneous mass of colorless crystals. Their X-ray structures were determined at 100 K.

The cocrystals with **DITCB** and **DITBB** both crystallized in the triclinic space group $P\overline{1}$, with one **DMAP** molecule and one half of the perhalobenzene in the asymmetric unit. In contrast, the cocrystal containing the bromoiodotetrafluorobenzene, **IBTFB**, crystallized in the monoclinic space group $P2_1/c$, as reported for the diiodotetrafluorobenzene, **DITFB**, cocrystal. The cocrystal with **DIBFB**, in which the perhalobenzene does not have twofold symmetry along the axis of the C—I bonds, crystallized in the triclinic space group $P\overline{1}$; however, the asymmetric unit included both **DMAP** moieties, as well as the complete halobenzene with two unique I···N halogen bonds.

Despite the variations in space group and asymmetric unit, the structures of the core 2:1 halogen-bonded cocrystals are similar, with each containing a central perhalobenzene halogen bonded to two 4-(dimethylamino)pyridine molecules that are twisted relative to the perhalobenzene (Fig. 2). Indeed, this arrangement is like that reported for the 2:1 cocrystal formed between **DMAP** and **DITFB**.

The shortest halogen-bond N···I separation in the structures reported herein is observed in the cocrystal with the iodobromotetrafluorobenzene **IBTFB** at 2.588 (5) Å, which is 73.3% of the sum of the van der Waals radii (Bondi, 1964). This is in accord with the slightly more positive σ-hole on the I atom as compared to tetrafluorodiodobenzene **DITFB** (Fig. 1). Somewhat surprisingly though, given the significantly lower molecular electrostatic potentials, the corresponding N···I separations for the diodotetrachloro and diiodotetrabromo analogues **DITCB** and **DITBB** are also relatively short at 76.4 and 76.7% of the sum of the van der Waals radii. A characteristic of halogen bonds is the near linear C—I···N angle and, for this group of structures, these angles range from 177.71 (18) to 179.5 (3)°. It is noteworthy that, in all of these structures, the flanking **DMAP** molecules are twisted relative to the central diiodoperhalobenzene at angles ranging from 76.3 (2) to 86.6 (16)°. The geometric parameters for the structures reported here are collated in Table 2, where the corresponding data for cocrystal **(DMAP)$_2$·DITFB** are also included for comparison.

To better understand the intermolecular relationships within the cocrystals of **DMAP** and each of **DITCB** and **DITBB**, the gross packing in each structure viewed along the *b* axis is shown in Fig. 3.

In each structure, pairs of **DMAP** molecules are sandwiched between the halobenzene rings, with a C—H···π interaction. The closest interactions to the centroid of the halobenzene are

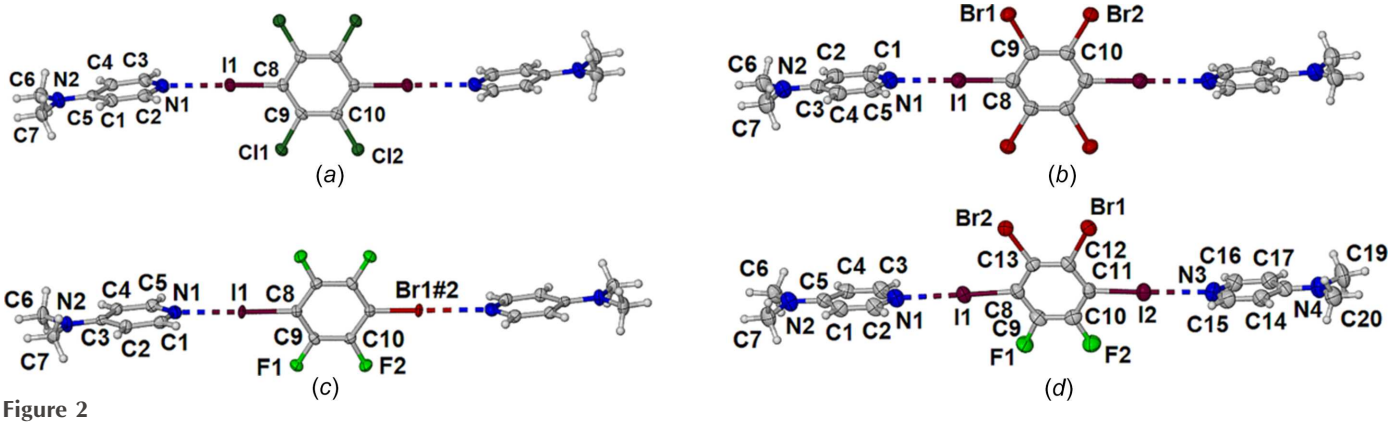

Figure 2
The asymmetric units of the 2:1 cocrystals reported in this article: (*a*) **(DMAP)$_2$·DITCB**; (*b*) **(DMAP)$_2$·DITBB**; (*c*) **(DMAP)$_2$·IBTFB**; (*d*) **(DMAP)$_2$·DIBFB**. For parts (*a*), (*b*), and (*c*), the full symmetry-generated perhalobenzene and second **DMAP** molecule are also shown for completeness. Displacement ellipsoids are drawn at the 70% probability level and halogen bonds are represented by dashed lines. The atoms are color coded as follows: C grey, N blue, Cl dark green, F bright green, Br red, and I maroon, and halogen bonds are shown as dashed lines.

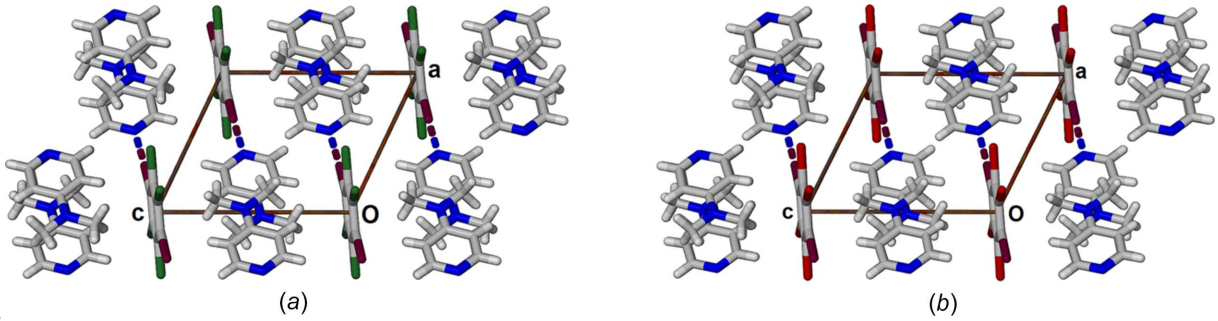

Figure 3
View along the *b* axis of the packing within cocrystals (*a*) **(DMAP)$_2$·DITCB** and (*b*) **(DMAP)$_2$·DITBB**. Halogen bonds are shown as dashed lines and atoms are color coded as in Fig. 2.

Table 2
Geometric parameters (Å, °) for the cocrystals in this study.

Perhalobenzene	**DITFB**[a]	**DITCB**	**DITBB**	**IBTFB**	**DIBFB**
N···I	2.6622 (4)	2.698 (4)	2.708 (5)	2.588 (5) I 2.797 (6) Br	2.675 (5) 2.707 (5)
C—I···N	179.323 (14)	178.08 (13)	178.48 (16)	179.5 (3)	178.11 (18) 177.71 (18)
C_p—N···I[b]	172.92 (2)	172.67 (17)	174.9 (2)	173.2 (2)	175.5 (3) 175.5 (3)
CX_6···**DMAP**	79.17 (2)	86.6 (16)	82.4 (5)	78.6 (4)	76.59 (19) 76.3 (2)

Notes: (*a*) data from CSD refcode RUYHID02 collected at 100 K (Wang *et al.*, 2018); (*b*) C_p is the pyridyl C atom *para* to the pyridyl N atom.

2.937 (5) and 2.916 (7) Å, with C—H···*Cg* angles (where *Cg* is the centroid of the pyridine ring) of 140.7 (5) and 132.60 (17)° for **DITCB** and **DITBB**, respectively. The more intimate nature of the intermolecular interactions within each structure is further shown in the views along the *c* axis in Fig. 4. This figure reveals that the **DMAP** molecules are π-stacked in pairs, with a head-to-tail orientation so that the centroid of one pyridine lies above the C atom *para* to the N atom of the second pyridyl ring. Pairs of these **DMAP** molecules are offset, with H···H methyl–methyl interactions. In cocrystal **(DMAP)$_2$·DITCB**, the perpendicular separation between these is 3.587 (2) Å, while in cocrystal **(DMAP)$_2$·DITBB**, the perpendicular separation is 3.566 (3) Å (Spek, 2020). There is a halogen–π interaction in each structure, labeled 'z' in Fig. 4, with distances to the centroids (*Cg*) of the respective pyridine rings of 3.643 (2) and 3.615 (3) Å, and C—*X*···*Cg* angles of 135.21 (16) and 132.60 (17)° for *X* = Cl in **DITCB** and *X* = Br in **DITBB**, respectively. The similarities between these structures in terms of geometric parameters (Table 1), space group, and unit-cell parameters (Table 2) and intermolecular interactions are striking, indicating that the structures of **(DMAP)$_2$·DITCB** and **(DMAP)$_2$·DITBB** are isomorphous.

The unit-cell packing in cocrystal **(DMAP)$_2$·IBTFB** is shown in Fig. 5. As can be seen, the stacked **DMAP** molecules are sandwiched between the perhalobenzene rings, with a close contact between H2 and the centroid of the perhalo ring of 2.787 (4) Å, and a C—H···*Cg* angle of 145.9 (3)° (where *Cg* is the centroid of the pyridine ring). Pairs of **DMAP** molecules π-stack head-to-tail with full overlap, labeled as 'y1' in Fig. 5(*b*), and a perpendicular separation of 3.5874 (17) Å. In contrast to the structures in Fig. 4, the pairs of π-stacked **DMAP** molecules are also slip-stacked, with significant overlap between the pyridyl rings, and have a centroid-to-centroid separation of 3.651 (2) Å, labeled as 'y2' in Fig. 5(*b*). Accordingly, there is no halogen–π interaction, as seen in Fig. 4. The closest F···F contact, at 2.803 (3) Å, is essentially equal to the sum of the van der Waals radii of 2.80 Å. Thus, in this structure, the principal difference with respect to **(DMAP)$_2$·DITCB** and **(DMAP)$_2$·DITBB** is that the pairs of head-to-tail π-stacked **DMAP** dimers have more overlap precluding, or due to the lack of, a halogen–π interaction. The structure of **(DMAP)$_2$·IBTFB** is isomorphous with the published structure of **(DMAP)$_2$·DITFB**.

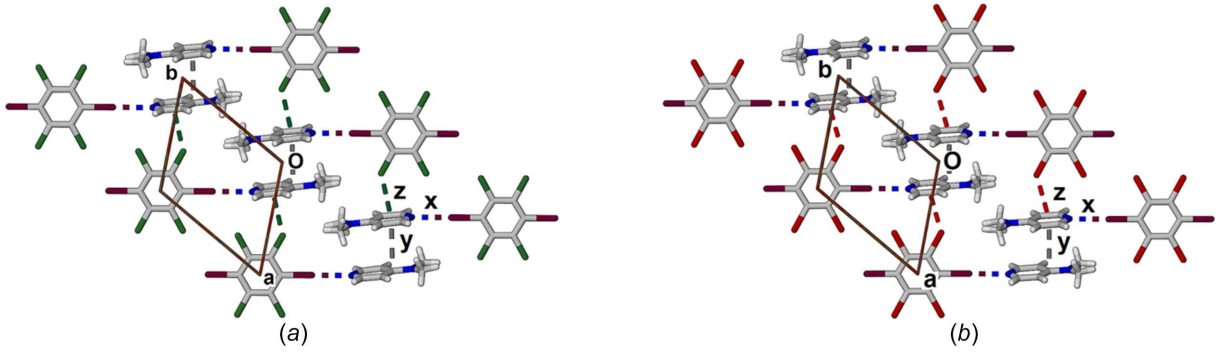

Figure 4
View along the *c* axis of the packing within cocrystals (*a*) **(DMAP)$_2$·DITCB** and (*b*) **(DMAP)$_2$·DITBB**. Halogen bonds are denoted as 'x', π–π interactions as 'y', and halogen–π interactions as 'z'.

Table 3
Hirshfeld analysis of the **DMAP** molecule in each 2:1 **(DMAP)$_2$·CI$_2$$X_4$** cocrystal with an element-by-element delineation of the % contribution.

XB donor	H···H^{a,b}	C···X^a	C···C^a	H···C^{a,b}	H···X^a	H···I^a	N···I^a
DITCB	35.5	3.3	3.4	20.9	17.6	7.7	3.0
DITBB	37.0	4.0	3.3	20.2	16.4	7.6	3.0
DIBFB	35.8	4.5 (Br) 0.0 (F)	3.4	20.3	16.0 (Br) 0.0 (F)	8.2	3.1
DITFB	34.3	0.0	5.3	21.3	17.5	8.2	3.0

Notes: (*a*) the first element listed corresponds to the DMAP molecule, while the second is an element with a close contact from outside the DMAP molecule. (*b*) Includes reciprocal contacts. Part corresponds to a DMAP methyl–H contact with the C atom of a π-stacked DMAP molecule and part corresponds to the DMAP pyridyl–H contact to a C atom of C_6X_6.

The packing in cocrystal **(DMAP)$_2$·DIBFB** along the *c* axis is shown in Fig. 6(*a*). Not surprisingly, the structure contains elements like those observed in cocrystal **(DMAP)$_2$·DITBB** and those observed in **(DMAP)$_2$·IBTFB**. Thus, the fluorine substituents in adjacent **DIBFB** molecules face towards each other [Fig. 6(*b*)]. The F···F contacts are essentially equal to the sum of the van der Waals radii. In contrast, the bromine substituent has a halogen–π interaction with a **DMAP** molecule, with a C—Br···*Cg* separation of 3.689 (2) Å, labeled 'z' in Fig. 6(*b*). The **DMAP** molecules form a four-molecule π-stack with two unique centroid-to-centroid distances of 3.945 (3) and 3.974 (3) Å, marked as 'y1' and 'y2' in Fig. 6(*b*). The stacking is head-to-tail throughout. In terms of the near orthogonal interaction between **DMAP** molecules and the perhalobenzene ring, there is a close pyridine–perhalobenzene C—H···π interaction. The distance between pyridine atom H4 and the centroid of the perhalobenzene ring is 2.838 (7) Å, with a C—H···*Cg* angle of 145.0 (6)°.

3.3. Hirshfeld surface analysis

A Hirshfeld surface analysis was performed for each component in each cocrystal along with a fingerprint analysis in which the surface contacts are filtered according to the elements inside and outside the surface. In Fig. 7, the fingerprint analysis corresponding to contacts with the surface of the **DMAP** molecule in cocrystal **(DMAP)$_2$·DITCB** are shown. It is noteworthy that the major contacts are H···H (35.5% of the **DMAP** surface area) that correspond to methyl–methyl interactions between offset pairs of **DMAP** molecules. The C···H contacts corresponding to 20.9% of the surface area correlate to the self-complementary methyl H-atom interactions with the C atoms *ortho* to the pyridine N atom. The N···I halogen bond as a single-point contact corresponds to just 3.0% of the surface area of the **DMAP** molecule. The secondary π–type halogen bond is manifest in the C···Cl contact at 3.3% of the **DMAP** surface area.

Similar fingerprint analysis of the Hirshfeld surface of the **DMAP** molecule in the analogous tetrabromo cocrystal **(DMAP)$_2$·DITBB** revealed an almost identical breakdown of atom-to-atom surface contacts. These data are collected in Table 3, along with data for the dibromodifluoro analogue **DIBFB** and, for comparison, data for **DITFB**. The latter is included as the Br/I disorder in the cocrystal **(DMAP)$_2$·IBTFB** precludes meaningful Hirshfeld surface analysis. It is noteworthy that most interactions have similar percentages with the exception that there is no C—F···C(π) interaction in the cocrystals with **DIBFB** and **DITFB**, whereas the chloro and bromo substituents have a C—Cl(Br)···C(π) contacts corresponding to 3.3–4.5% of the **DMAP** surface area.

In Fig. 8, the element-to-element fingerprint analysis corresponding to the central **DITCB** molecule in cocrystal **(DMAP)$_2$·DITCB** is shown. The major intermolecular contacts are Cl···H (37.2% of the **DITCB** surface area) and I···H (26.5%) that correspond to interactions of each halogen with the **DMAP** methyl H atoms. The C···H interaction (16.0%) corresponds to the pyridyl-ring H atoms nearly perpendicular C—H···π interaction with the perhalobenzene. The I···N

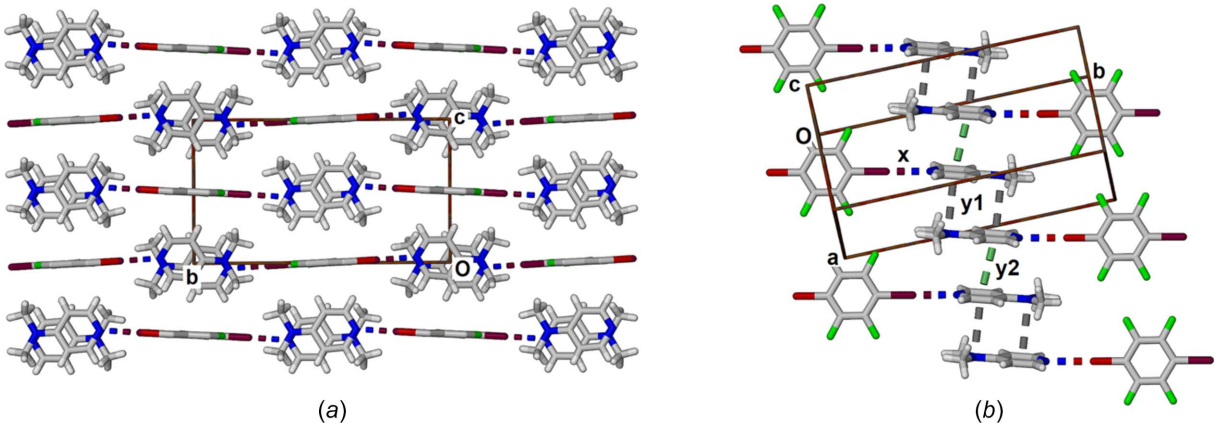

Figure 5
View along the *a* axis of the packing within cocrystal **(DMAP)$_2$·IBTFB**. Atoms are color coded as before, with halogen bonds as dashed lines. (*b*) Oblique view of the same structure showing the head-to-tail π-stacking of **DMAP** molecules, with full overlapped pairs labeled 'y1' and partial overlapped pairs labeled 'y2'. Halogen bonds are labeled 'x'.

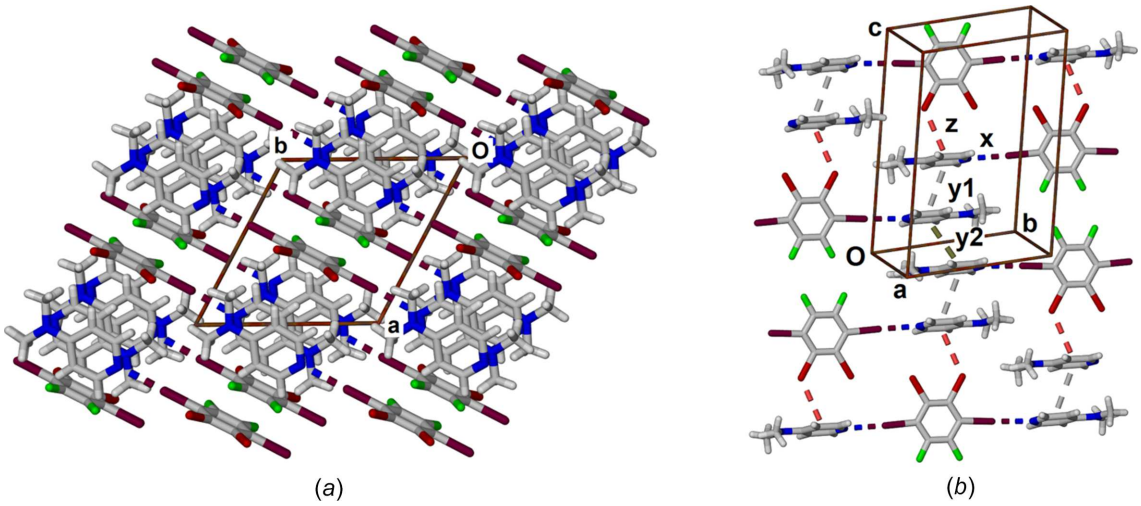

(*a*) (*b*)

Figure 6
View along the *c* axis of the packing within cocrystal **(DMAP)$_2$·DIBFB**. Atoms are color coded as before, with halogen bonds as dashed lines. (*b*) Oblique view showing head-to-tail π-stacking of **DMAP** molecules, with pairs labeled 'y1' and 'y2'. The I···N halogen bond is labeled 'x' and the C—Br···π halogen bond is labeled 'z'.

Table 4
Hirshfeld analysis of the perhalobenzene molecule in each 2:1 **(DMAP)$_2$·-Cl$_2$X$_4$** cocrystal with an element-by-element delineation of the % contribution.

XB donor	*X*···H[a]	I···H	C···H	*X*···*X*	I···*X*[b]	I···N
DITCB	37.2	26.5	16.0	4.3	3.9	5.3
DITBB	36.0	25.1	15.9	5.8	3.9	5.0
DIBFB	19.0 (Br)	29.9	16.0	3.8 (Br)	2.1 (Br)	5.4
	15.5 (F)			3.3 (F)	0.0 (F)	
DITFB	34.6	35.1	16.6	7.4	0.0	6.2

Notes: (*a*) the first element listed corresponds to the Cl$_2$X$_4$ molecule, while the second is an element with a close contact from outside the Cl$_2$X$_4$ molecule; (*b*) includes reciprocal contacts.

contact only amounts to 5.3% of the surface of the perhalobenzene.

The corresponding analyses of the cocrystals with the bromo analogue **DITBB**, the bromofluoro analogue **DIBFB**, and the tetrafluoro analogue **DITFB** are collated in Table 4. The first three entries include I···*X* interactions, corresponding to the offset stacking of pairs of **DMAP** molecules [Fig. 4(*b*)], whereas the latter two entries do not have this interaction for the F-atom substituents since the **DMAP** molecules are more uniformly π-stacked facilitating F···F contacts [Figs. 5(*b*) and 6(*b*)].

3.4. Intermolecular interaction energies

Structural analysis suggests that the role of halogen–π interactions in cocrystals **(DMAP)$_2$·DITCB** and **(DMAP)$_2$·-DITBB** is important in the subtle changes in crystal packing as

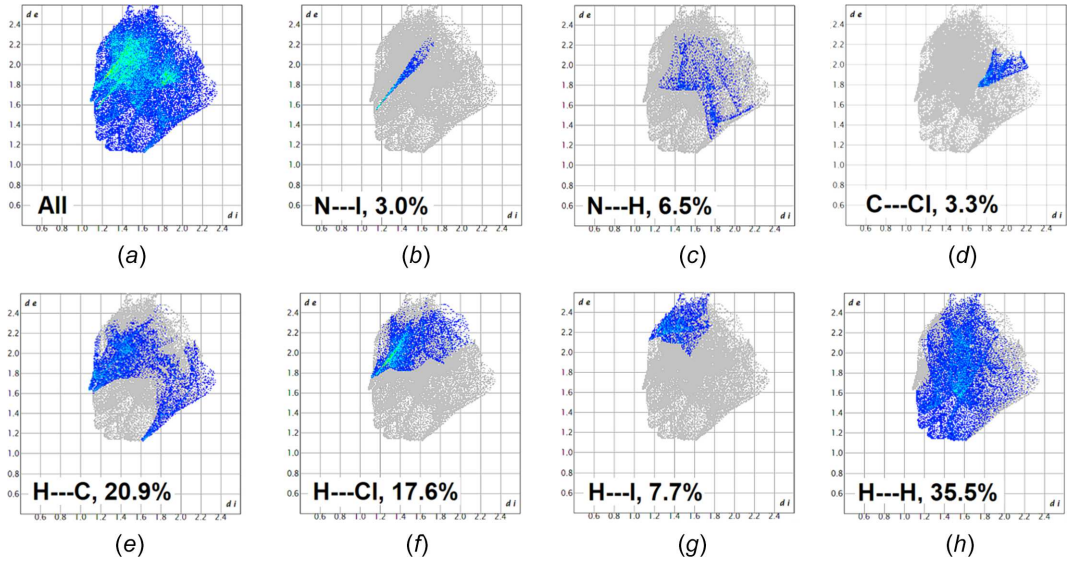

(*a*) (*b*) (*c*) (*d*)
(*e*) (*f*) (*g*) (*h*)

Figure 7
2D fingerprint plots showing the percentage contributions of the major interactions to the total Hirshfeld surface area of **DMAP** in cocrystal **(DMAP)$_2$·-DITCB**, showing (*a*) all, (*b*) N···I, (*c*) N···H, (*d*) C···C/C···C, (*e*) H···C/C···H, (*f*) H···Cl, (*g*) H···I, and (*h*) H···H. Note that parts (*c*), (*d*), (*e*), and (*h*) include reciprocal interactions. Not shown are N···C (0.1%), N···Cl (1.5%), and N···N (0.5%).

Table 5
Major intermolecular interaction energies between interacting molecules within each cocrystal listed according to the major interaction type for each pair of molecules.

Halobenzene major interaction	**DITCB**	**DITBB**	**DIBFB**
DMAP π–π stacking[a]	−36.8	−36.9	−37.0, −36.9[d]
DMAP offset π–π stacked[b]	−15.4	−13.8	−12.8
Halogen bond (N···I)[c]	−29.9 (76.4)	−29.5 (76.7)	−32.2 (75.8, 76.6)
C—H···π (C_6X_6)	−19.7	−22.0	−21.1
C—X···π (**DMAP**)	−9.6	−15.4	−15.9 (X = Br)

Notes: (*a*) corresponds to pairs of DMAP molecules with maximum π–π overlap. (*b*) Mainly methyl–methyl interactions. (*c*) N···I separation as a % of the van der Waals radii in parentheses. (*d*) The second value corresponds to the inner two DMAP molecules, labeled 'y2' in Fig. 6(*b*).

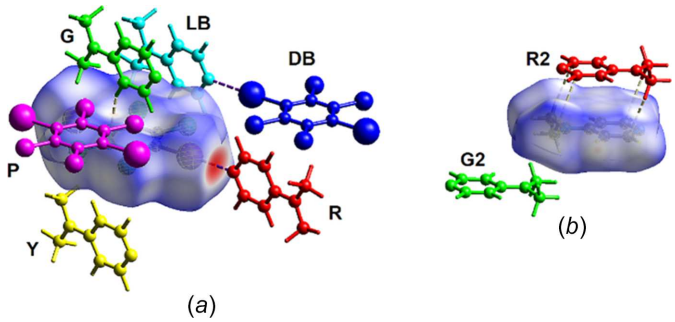

Figure 9
(*a*) Color-coded molecules, within 3.8Å of a central **DITCB** molecule, in cocrystal **(DMAP)$_2$·DITCB**, that have significant attractive intermolecular energies of interaction. The molecule color and labels are: R (red), DB (dark blue), G (green), R (red), LB (light blue), and P (pink). (*b*) Color-coded **DMAP** molecules that have close interactions with the unique **DMAP** molecule in cocrystal **(DMAP)$_2$·DITCB**. The color codes are: R2 (red) and G2 (green).

compared to the corresponding cocrystals **(DMAP)$_2$·DITFB** and **(DMAP)$_2$·IBTFB**. *CrystalExplorer21* was used to calculate the intermolecular energy between molecules for each crystal structure. For **(DMAP)$_2$·DITCB**, this analysis focused first on the group of molecules within 3.80 Å of a central **DITCB** molecule and identified the most energetically favorable interactions. With respect to the **DITCB** molecule, the halogen-bonded molecule colored red, and labeled 'R' in Fig. 9(*a*), has the strongest interaction at −29.9 kJ mol^{-1}. The **DMAP** molecule (green and labeled 'G'), that is almost orthogonal and has C—H···π interactions with the perhalobenzene, has an interaction energy of −19.7 kJ mol^{-1}, while the second orthogonal molecule (yellow and labeled 'Y'), that has an C—H···Cl interaction, has an intermolecular interaction energy of −15.4 kJ mol^{-1}. The central **DITCB** molecule has a C—Cl···π interaction with the light-blue (LB) **DMAP** molecule, with an interaction energy of −9.6 kJ mol^{-1}. The two **DITCB** molecules that have the closest contacts to the central molecule have weak I···Cl (dark blue and labeled 'DB') and offset Cl···Cl interactions (pink and labeled 'P') with the central molecule, with interaction energies of −7.3 and −5.1 kJ mol^{-1}, respectively. To provide a further understanding of the subtlety in packing within the cocrystal, the interaction energy between π-stacked **DMAP** molecules was also determined. This, shown graphically in Fig. 9(*b*), revealed that the head-to-tail packed **DMAP** molecules [red and labeled 'R2' in Fig. 9(*b*)] have the strongest intermolecular interaction energy in the cocrystal of −36.8 kJ mol^{-1}, while the offset **DMAP** molecule [green and labeled 'G2' in Fig. 9(*b*)], that has a dispersive methyl–methyl interaction, has an overall intermolecular interaction energy of −15.4 kJ mol^{-1}.

A similar analysis was performed for cocrystals **(DMAP)$_2$·DITBB** and **(DMAP)$_2$·DIBFB.** The major interaction energies for this group of cocrystals are collated in Table 5. Consistently across all three structures, the strongest intermolecular interaction is the head-to-tail π-stacked **DMAP** molecules with attractive energies of interaction from −36.8 to

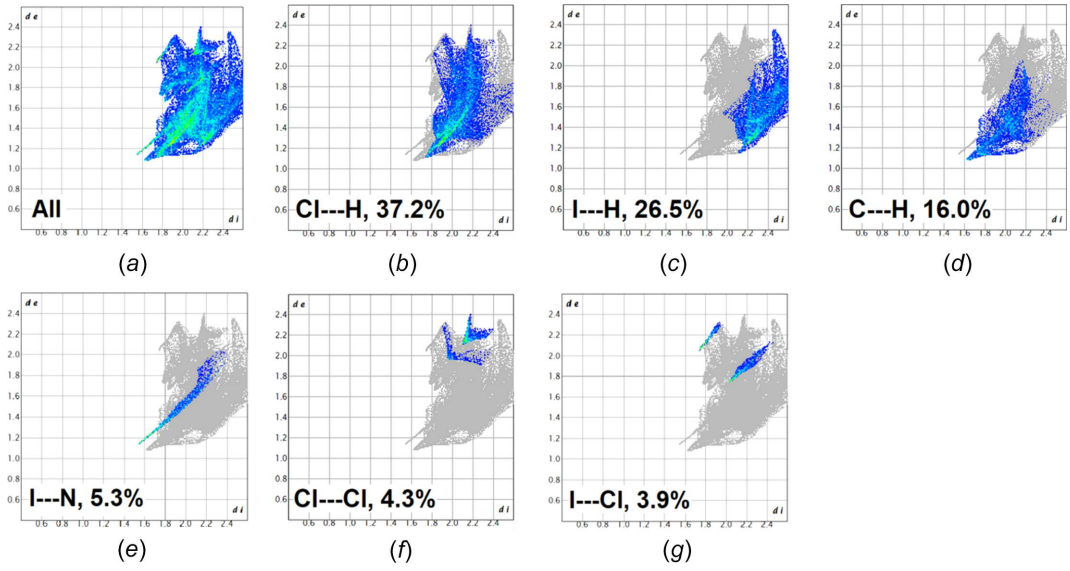

Figure 8
2D fingerprint plots showing the percentage contributions of the major interactions to the total Hirshfeld surface area of **DITCB** in cocrystal **(DMAP)$_2$·DITCB**, showing (*a*) all, (*b*) Cl···H, (*c*) I···H, (*d*) C···H, (*e*) I···N, (*f*) Cl···Cl, and (*g*) I···Cl/Cl···I. Not shown is Cl···N (2.5%).

38.6 kJ mol^{-1}. The halogen bond is the second strongest intermolecular interaction in all the structures, with the strongest interaction being for **DIBFB** and the weakest for **DITBB**, in line with the decreasing electronegativity of the halogen-bonded halogen atom. The **DMAP** C—H$\cdots\pi$ interaction to the perhalobenzene is the third strongest intermolecular interaction in all three structures.

4. Conclusions

The structures of a series of 2:1 cocrystals formed between 4-(dimethylamino)pyridine and perhalobenzenes, that are considered ditopic *n*-type halogen-bond donors, all have a similar three-molecule halogen-bonded core. In this core, each perhalobenzene is halogen bonded to two dimethylaminopyridines that are almost orthogonal to the central benzene ring. There are subtle differences in the packing within the crystals and these differences are rationalized in terms of the ability of the perhalobenzene to participate in weaker secondary interactions. Thus, in each of the cocrystals formed with 1,2,4,5-tetrachloro-3,6-diiodobenzene and 1,2,4,5-tetrabromo-3,6-diiodobenzene, the I atom is the best halogen-bond donor. However, the Cl and Br atoms both support the formation of a weak secondary halogen–π interactions to 4-(dimethylamino)pyridine molecules. This secondary interaction is absent in the cocrystal formed with 1-bromo-2,3,5,6-tetrafluoro-4-iodobenzene, where F$\cdots$F contacts are present. The cocrystal formed with 1,2-dibromo-4,5-difluoro-3,6-diiodobenzene exhibits both the weak secondary halogen–π interaction and F$\cdots$F contacts. The cocrystals with 1,2,4,5-tetrachloro-3,6-diiodobenzene and 1,2,4,5-tetrabromo-3,6-diiodobenzene were found to be isomorphous.

Acknowledgements

EB and NB thank the National Science Foundation for financial support of this research and EB acknowledges The National Science Foundation, Division of Chemistry, Major Research Instrumentation Program that funded the purchase of the Synergy-S X-ray diffractometer.

Funding information

Funding for this research was provided by: National Science Foundation, Directorate for Mathematical and Physical Sciences (grant No. CHE1903593 to Eric Bosch; grant No. CHE1903581 to Nathan P. Bowling); National Science Foundation, Directorate for Mathematical and Physical Sciences (award No. 2117129 to Eric Bosch).

References

Aakeroy, C. B., Chopade, P. D. & Desper, J. (2013). *Cryst. Growth Des.* **13**, 4145–4150.
Barbour, L. J. (2020). *J. Appl. Cryst.* **53**, 1141–1146.
Bennion, J. C., Vogt, L., Tuckerman, M. E. & Matzger, A. J. (2016). *Cryst. Growth Des.* **16**, 4688–4693.
Bondi, A. (1964). *J. Phys. Chem.* **68**, 441–451.
Bosch, E., Kruse, S. J., Krueger, H. R. Jr & Groeneman, R. H. (2019). *Cryst. Growth Des.* **19**, 3092–3096.
Bourhis, L. J., Dolomanov, O. V., Gildea, R. J., Howard, J. A. K. & Puschmann, H. (2015). *Acta Cryst.* A**71**, 59–75.
Cavallo, G., Metrangolo, P., Milani, R., Pilati, T., Priimagi, A., Resnati, G. & Terraneo, G. (2016). *Chem. Rev.* **116**, 2478–2601.
Chen, Y.-H., Zhang, G. Z., Chen, F. H., Zhang, S. Q., Fang, X., Chen, H. M. & Lin, M. J. (2024). *Chem. Sci.* **15**, 7659–7666.
Clark, R. C. & Reid, J. S. (1995). *Acta Cryst.* A**51**, 887–897.
Costa, P. J. (2017). *Phys. Sci. Rev.* **2**, 20170136.
Desiraju, G. R., Ho, P. S., Kloo, L., Legon, A. C., Marquardt, R., Metrangolo, P., Politzer, P., Resnati, G. & Rissanen, K. (2013). *Pure Appl. Chem.* **85**, 1711–1713.
Dolomanov, O. V., Bourhis, L. J., Gildea, R. J., Howard, J. A. K. & Puschmann, H. (2009). *J. Appl. Cryst.* **42**, 339–341.
Gilday, L. C., Robinson, S. W., Barendt, T. A., Langton, M. J., Mullaney, B. R. & Beer, P. D. (2015). *Chem. Rev.* **115**, 7118–7195.
Groom, C. R., Bruno, I. J., Lightfoot, M. P. & Ward, S. C. (2016). *Acta Cryst.* B**72**, 171–179.
LG Limited (2019). Republic of Korea Patent No. KR2019062252 A 2019-06-05.
Lu, J., Ho, D. M., Vogelaar, N. J., Kraml, C. M. & Pascal, R. A. (2004). *J. Am. Chem. Soc.* **126**, 11168–11169.
Panikkattu, V., Huber, A. S., Sinha, A. S., Averkiev, B. B. & Aakeröy, C. B. (2022). *Cryst. Growth Des.* **22**, 1538–1542.
Politzer, P., Murray, J. S. & Clark, T. (2010). *Phys. Chem. Chem. Phys.* **12**, 7748–7757.
Präsang, C., Whitwood, A. C. & Bruce, D. W. (2009). *Cryst. Growth Des.* **9**, 5319–5326.
Quentin, J. & MacGillivray, L. R. (2020). *Cryst. Growth Des.* **20**, 7501–7515.
Reddy, C. M., Kirchner, M. T., Gundakaram, R. C., Padmanabhan, K. A. & Desiraju, G. R. (2006). *Chem. A Eur. J.* **12**, 2222–2234.
Rigaku OD (2023). *CrysAlis PRO*. Rigaku Oxford Diffraction, Yarnton, Oxfordshire, England.
Roper, L. C., Präsang, C., Kozhevnikov, V. N., Whitwood, A. C., Karadakov, P. B. & Bruce, D. W. (2010). *Cryst. Growth Des.* **10**, 3710–3720.
Sheldrick, G. M. (2015). *Acta Cryst.* A**71**, 3–8.
Spackman, P. R., Turner, M. J., McKinnon, J. J., Wolff, S. K., Grimwood, D. J., Jayatilaka, D. & Spackman, M. A. (2021). *J. Appl. Cryst.* **54**, 1006–1011.
Spek, A. L. (2020). *Acta Cryst.* E**76**, 1–11.
Wang, R., Hartnick, D. & Englert, U. (2018). *Z. Kristallogr. Cryst. Mater.* **233**, 733–744.
Wavefunction (2022). *SPARTAN'20*. Wavefunction Inc., Irvine, CA, USA.

supporting information

Acta Cryst. (2024). C**80**, 553-561 [https://doi.org/10.1107/S205322962400771X]

Role of secondary interactions in a series of 2:1 halogen-bonded cocrystals formed between 4-(dimethylamino)pyridine and ditopic halogen-bond donors

Eric Bosch and Nathan P. Bowling

Computing details

4-(Dimethylamino)pyridine–1,2,4,5-tetrachloro-3,6-diiodobenzene (2/1) (2DMAP.DITCB)

Crystal data

$2C_7H_{10}N_2{\cdot}C_6Cl_4I_2$
M_r = 712.03
Triclinic, $P\overline{1}$
a = 8.1680 (3) Å
b = 9.1290 (4) Å
c = 9.8118 (3) Å
α = 103.727 (3)°
β = 107.165 (3)°
γ = 112.180 (4)°
V = 594.91 (5) Å^3
Z = 1
$F(000)$ = 344.569
D_x = 1.987 Mg m^{-3}
Cu $K\alpha$ radiation, λ = 1.54184 Å
Cell parameters from 5533 reflections
θ = 5.2–76.7°
μ = 25.03 mm^{-1}
T = 100 K
Block, colourless
0.14 × 0.1 × 0.03 mm

Data collection

Rigaku XtaLAB Synergy Dualflex diffractometer with a HyPix detector
Radiation source: micro-focus sealed X-ray tube, PhotonJet (Cu) X-ray Source
Mirror monochromator
Detector resolution: 10.0000 pixels mm^{-1}
ω scans
Absorption correction: analytical (CrysAlis PRO; Rigaku OD, 2023)
T_{min} = 0.104, T_{max} = 0.510
8921 measured reflections
2500 independent reflections
2413 reflections with $I \geq 2u(I)$
R_{int} = 0.063
θ_{max} = 77.8°, θ_{min} = 5.1°
h = −8→10
k = −11→11
l = −12→10

Refinement

Refinement on F^2
Least-squares matrix: full
$R[F^2 > 2\sigma(F^2)]$ = 0.038
$wR(F^2)$ = 0.107
S = 1.02
2500 reflections
138 parameters
0 restraints
16 constraints
Primary atom site location: dual
H-atom parameters constrained
$w = 1/[\sigma^2(F_o^2) + (0.0833P)^2]$ where $P = (F_o^2 + 2F_c^2)/3$
$(\Delta/\sigma)_{max}$ = −0.0004
$\Delta\rho_{max}$ = 1.33 e Å^{-3}
$\Delta\rho_{min}$ = −1.51 e Å^{-3}

Fractional atomic coordinates and isotropic or equivalent isotropic displacement parameters (Å²)

	x	y	z	U_{iso}*/U_{eq}
I1	0.66832 (3)	0.55170 (3)	0.83016 (2)	0.02027 (14)

Cl1	0.55433 (14)	0.87164 (13)	0.82188 (12)	0.0244 (2)
Cl2	0.84204 (14)	1.25822 (12)	0.96798 (12)	0.0236 (2)
N1	0.4176 (6)	0.2104 (5)	0.6920 (5)	0.0256 (8)
N2	−0.0264 (6)	−0.3045 (5)	0.4505 (5)	0.0265 (8)
C10	0.9318 (6)	1.1168 (5)	0.9868 (5)	0.0191 (7)
C2	0.3727 (6)	0.1184 (6)	0.5449 (5)	0.0250 (8)
H2	0.4439 (6)	0.1742 (6)	0.4948 (5)	0.0299 (10)*
C5	0.1183 (6)	−0.1363 (5)	0.5291 (5)	0.0206 (8)
C9	0.8010 (6)	0.9401 (5)	0.9196 (5)	0.0197 (7)
C1	0.2313 (6)	−0.0503 (6)	0.4621 (5)	0.0246 (8)
H1	0.2100 (6)	−0.1089 (6)	0.3594 (5)	0.0295 (10)*
C3	0.3125 (6)	0.1261 (5)	0.7584 (5)	0.0240 (8)
H3	0.3424 (6)	0.1869 (5)	0.8631 (5)	0.0287 (10)*
C8	0.8668 (6)	0.8202 (5)	0.9319 (5)	0.0197 (8)
C4	0.1660 (6)	−0.0410 (6)	0.6849 (5)	0.0233 (8)
H4	0.0967 (6)	−0.0928 (6)	0.7379 (5)	0.0280 (10)*
C6	−0.1438 (7)	−0.3878 (6)	0.5229 (6)	0.0297 (9)
H6a	−0.0579 (8)	−0.381 (4)	0.621 (2)	0.0445 (14)*
H6b	−0.218 (4)	−0.330 (3)	0.544 (4)	0.0445 (14)*
H6c	−0.234 (4)	−0.5088 (14)	0.453 (2)	0.0445 (14)*
C7	−0.0832 (7)	−0.3915 (6)	0.2866 (5)	0.0287 (9)
H7a	−0.119 (5)	−0.325 (3)	0.2303 (8)	0.0431 (13)*
H7b	0.027 (2)	−0.402 (4)	0.2728 (6)	0.0431 (13)*
H7c	−0.195 (4)	−0.5064 (19)	0.2461 (12)	0.0431 (13)*

Atomic displacement parameters (Å²)

	U^{11}	U^{22}	U^{33}	U^{12}	U^{13}	U^{23}
I1	0.01750 (18)	0.01770 (19)	0.02180 (19)	0.00611 (13)	0.00822 (13)	0.00595 (13)
Cl1	0.0153 (4)	0.0225 (5)	0.0289 (5)	0.0072 (4)	0.0055 (4)	0.0081 (4)
Cl2	0.0205 (5)	0.0205 (5)	0.0285 (5)	0.0109 (4)	0.0086 (4)	0.0084 (4)
N1	0.0211 (18)	0.0238 (18)	0.0272 (19)	0.0105 (15)	0.0079 (15)	0.0063 (16)
N2	0.0226 (18)	0.0239 (18)	0.0230 (18)	0.0053 (15)	0.0093 (15)	0.0040 (15)
C10	0.0201 (19)	0.0204 (18)	0.0195 (18)	0.0102 (16)	0.0113 (16)	0.0082 (15)
C2	0.021 (2)	0.029 (2)	0.029 (2)	0.0129 (18)	0.0130 (18)	0.0147 (18)
C5	0.0157 (19)	0.0203 (19)	0.024 (2)	0.0101 (16)	0.0052 (16)	0.0067 (16)
C9	0.0153 (17)	0.0236 (19)	0.0149 (18)	0.0065 (15)	0.0051 (14)	0.0054 (15)
C1	0.022 (2)	0.025 (2)	0.025 (2)	0.0124 (17)	0.0097 (17)	0.0058 (17)
C3	0.0191 (19)	0.023 (2)	0.026 (2)	0.0087 (17)	0.0091 (17)	0.0068 (17)
C8	0.0178 (19)	0.0172 (18)	0.021 (2)	0.0058 (16)	0.0089 (16)	0.0066 (16)
C4	0.0199 (19)	0.026 (2)	0.024 (2)	0.0120 (17)	0.0096 (17)	0.0097 (17)
C6	0.027 (2)	0.027 (2)	0.032 (2)	0.0087 (19)	0.013 (2)	0.014 (2)
C7	0.025 (2)	0.021 (2)	0.025 (2)	0.0063 (17)	0.0052 (18)	0.0006 (17)

Geometric parameters (Å, º)

I1—C8	2.125 (4)	C5—C4	1.417 (6)
Cl1—C9	1.730 (4)	C9—C8	1.405 (6)

Cl2—C10	1.728 (4)	C1—H1	0.9500
N1—C2	1.343 (6)	C3—H3	0.9500
N1—C3	1.350 (6)	C3—C4	1.367 (6)
N2—C5	1.371 (6)	C4—H4	0.9500
N2—C6	1.453 (6)	C6—H6a	0.9800
N2—C7	1.451 (6)	C6—H6b	0.9800
C10—C9	1.398 (6)	C6—H6c	0.9800
C10—C8^{i}	1.402 (6)	C7—H7a	0.9800
C2—H2	0.9500	C7—H7b	0.9800
C2—C1	1.370 (6)	C7—H7c	0.9800
C5—C1	1.398 (6)		

C3—N1—C2	115.7 (4)	C4—C3—N1	124.3 (4)
C6—N2—C5	120.4 (4)	C4—C3—H3	117.8 (3)
C7—N2—C5	119.7 (4)	C10^{i}—C8—I1	121.0 (3)
C7—N2—C6	119.2 (4)	C9—C8—I1	121.2 (3)
C9—C10—Cl2	119.0 (3)	C9—C8—C10^{i}	117.8 (4)
C8^{i}—C10—Cl2	119.9 (3)	C3—C4—C5	119.5 (4)
C8^{i}—C10—C9	121.1 (4)	H4—C4—C5	120.3 (2)
H2—C2—N1	117.8 (2)	H4—C4—C3	120.3 (3)
C1—C2—N1	124.4 (4)	H6a—C6—N2	109.5
C1—C2—H2	117.8 (3)	H6b—C6—N2	109.5
C1—C5—N2	122.1 (4)	H6b—C6—H6a	109.5
C4—C5—N2	121.8 (4)	H6c—C6—N2	109.5
C4—C5—C1	116.1 (4)	H6c—C6—H6a	109.5
C10—C9—Cl1	118.5 (3)	H6c—C6—H6b	109.5
C8—C9—Cl1	120.4 (3)	H7a—C7—N2	109.5
C8—C9—C10	121.1 (4)	H7b—C7—N2	109.5
C5—C1—C2	119.9 (4)	H7b—C7—H7a	109.5
H1—C1—C2	120.1 (3)	H7c—C7—N2	109.5
H1—C1—C5	120.1 (2)	H7c—C7—H7a	109.5
H3—C3—N1	117.8 (3)	H7c—C7—H7b	109.5

I1—C8—C10^{i}—Cl2^{i}	−0.2 (3)	Cl2—C10—C8^{i}—C9^{i}	179.9 (3)
I1—C8—C10^{i}—C9^{i}	−179.9 (3)	N1—C2—C1—C5	2.1 (5)
I1—C8—C9—Cl1	0.6 (3)	N1—C3—C4—C5	0.5 (5)
I1—C8—C9—C10	179.9 (3)	N2—C5—C1—C2	179.3 (4)
Cl1—C9—C10—Cl2	−0.6 (3)	N2—C5—C4—C3	179.5 (4)
Cl1—C9—C10—C8^{i}	179.7 (3)	C10—C9—C8—C10^{i}	−0.4 (4)
Cl1—C9—C8—C10^{i}	−179.7 (3)	C10^{i}—C8—C9—C10	−0.4 (4)
Cl2—C10—C9—C8	−179.9 (3)	C2—C1—C5—C4	−2.6 (5)

Symmetry code: (i) −*x*+2, −*y*+2, −*z*+2.

4-(Dimethylamino)pyridine–1,2,4,5-tetrabromo-3,6-diiodobenzene (2/1) (2DMAP.DITBB)

Crystal data

$2C_7H_{10}N_2{\cdot}C_6Br_4I_2$
$M_r = 889.83$
Triclinic, $P\overline{1}$
$a = 8.3361$ (2) Å
$b = 9.3089$ (3) Å
$c = 9.8204$ (2) Å
$\alpha = 102.484$ (2)°
$\beta = 108.399$ (2)°
$\gamma = 113.064$ (2)°
$V = 612.84$ (4) Å^3
$Z = 1$
$F(000) = 412.446$
$D_x = 2.411$ Mg m^{-3}
Cu $K\alpha$ radiation, $\lambda = 1.54184$ Å
Cell parameters from 8887 reflections
$\theta = 5.1$–$76.2°$
$\mu = 27.92$ mm^{-1}
$T = 100$ K
Irregular, clear colourless
0.21 × 0.17 × 0.08 mm

Data collection

Rigaku XtaLAB Synergy Dualflex diffractometer with a HyPix detector
Radiation source: micro-focus sealed X-ray tube, PhotonJet (Cu) X-ray Source
Mirror monochromator
Detector resolution: 10.0000 pixels mm^{-1}
ω scans
Absorption correction: analytical (CrysAlis PRO; Rigaku OD, 2023)
$T_{min} = 0.011$, $T_{max} = 0.146$
11315 measured reflections
2446 independent reflections
2429 reflections with $I \geq 2u(I)$
$R_{int} = 0.055$
$\theta_{max} = 77.1°$, $\theta_{min} = 5.2°$
$h = -10 \rightarrow 10$
$k = -8 \rightarrow 11$
$l = -12 \rightarrow 11$

Refinement

Refinement on F^2
Least-squares matrix: full
$R[F^2 > 2\sigma(F^2)] = 0.039$
$wR(F^2) = 0.110$
$S = 1.03$
2446 reflections
138 parameters
0 restraints
16 constraints
Primary atom site location: dual
H-atom parameters constrained
$w = 1/[\sigma^2(F_o^2) + (0.0862P)^2 + 0.8994P]$ where $P = (F_o^2 + 2F_c^2)/3$
$(\Delta/\sigma)_{max} = 0.001$
$\Delta\rho_{max} = 1.81$ e Å^{-3}
$\Delta\rho_{min} = -1.59$ e Å^{-3}

Fractional atomic coordinates and isotropic or equivalent isotropic displacement parameters (Å²)

	x	*y*	*z*	U_{iso}*/U_{eq}
I1	0.66402 (4)	0.55739 (3)	0.82970 (3)	0.02993 (15)
Br1	1.15967 (7)	0.73203 (6)	1.03222 (6)	0.03016 (17)
Br2	1.46760 (7)	1.13485 (6)	1.18536 (6)	0.03136 (17)
N1	0.4123 (7)	0.2193 (6)	0.6942 (6)	0.0353 (10)
N2	−0.0154 (7)	−0.2952 (6)	0.4640 (6)	0.0353 (10)
C9	1.0645 (7)	0.8856 (6)	1.0133 (6)	0.0272 (9)
C10	1.1981 (7)	1.0596 (6)	1.0791 (6)	0.0275 (9)
C3	0.1231 (7)	−0.1283 (6)	0.5382 (6)	0.0288 (10)
C8	0.8650 (7)	0.8220 (6)	0.9320 (6)	0.0276 (10)
C2	0.1625 (8)	−0.0294 (7)	0.6879 (6)	0.0326 (10)
H2	0.0909 (8)	−0.0788 (7)	0.7395 (6)	0.0391 (12)*
C4	0.2372 (8)	−0.0440 (7)	0.4711 (6)	0.0331 (10)
H4	0.2183 (8)	−0.1031 (7)	0.3705 (6)	0.0398 (12)*
C5	0.3767 (8)	0.1251 (7)	0.5530 (6)	0.0318 (10)

H5	0.4529 (8)	0.1783 (7)	0.5058 (6)	0.0381 (12)*
C1	0.3051 (8)	0.1395 (6)	0.7594 (6)	0.0313 (10)
H1	0.3289 (8)	0.2028 (6)	0.8605 (6)	0.0375 (12)*
C6	−0.1347 (9)	−0.3752 (7)	0.5351 (7)	0.0389 (12)
H6a	−0.0505 (9)	−0.362 (6)	0.638 (3)	0.0583 (18)*
H6b	−0.213 (6)	−0.322 (4)	0.546 (6)	0.0583 (18)*
H6c	−0.221 (5)	−0.4962 (15)	0.469 (3)	0.0583 (18)*
C7	−0.0661 (9)	−0.3860 (7)	0.3027 (7)	0.0415 (13)
H7a	−0.103 (7)	−0.326 (4)	0.2392 (13)	0.0623 (19)*
H7b	0.046 (3)	−0.392 (6)	0.2968 (11)	0.0623 (19)*
H7c	−0.175 (5)	−0.501 (2)	0.264 (2)	0.0623 (19)*

Atomic displacement parameters (Å²)

	U^{11}	U^{22}	U^{33}	U^{12}	U^{13}	U^{23}
I1	0.0289 (2)	0.0298 (2)	0.0321 (2)	0.01458 (16)	0.01462 (16)	0.01236 (15)
Br1	0.0299 (3)	0.0301 (3)	0.0361 (3)	0.0184 (2)	0.0154 (2)	0.0147 (2)
Br2	0.0245 (3)	0.0328 (3)	0.0362 (3)	0.0150 (2)	0.0118 (2)	0.0135 (2)
N1	0.032 (2)	0.034 (2)	0.035 (2)	0.0144 (19)	0.0144 (19)	0.0111 (19)
N2	0.036 (2)	0.037 (2)	0.032 (2)	0.016 (2)	0.018 (2)	0.0133 (19)
C9	0.029 (2)	0.031 (2)	0.029 (2)	0.0178 (19)	0.016 (2)	0.0135 (18)
C10	0.025 (2)	0.031 (2)	0.028 (2)	0.0134 (18)	0.0143 (19)	0.0132 (18)
C3	0.026 (2)	0.030 (2)	0.031 (2)	0.0150 (19)	0.012 (2)	0.0119 (19)
C8	0.031 (2)	0.028 (2)	0.025 (2)	0.0141 (19)	0.014 (2)	0.0108 (18)
C2	0.029 (2)	0.040 (3)	0.035 (3)	0.020 (2)	0.016 (2)	0.018 (2)
C4	0.031 (2)	0.041 (3)	0.032 (2)	0.020 (2)	0.015 (2)	0.015 (2)
C5	0.031 (2)	0.036 (2)	0.037 (3)	0.019 (2)	0.020 (2)	0.019 (2)
C1	0.033 (3)	0.031 (2)	0.032 (2)	0.017 (2)	0.016 (2)	0.011 (2)
C6	0.034 (3)	0.037 (3)	0.039 (3)	0.013 (2)	0.014 (2)	0.015 (2)
C7	0.042 (3)	0.034 (3)	0.038 (3)	0.014 (2)	0.017 (3)	0.006 (2)

Geometric parameters (Å, º)

I1—C8	2.126 (5)	C2—H2	0.9500
Br1—C9	1.902 (5)	C2—C1	1.382 (8)
Br2—C10	1.897 (5)	C4—H4	0.9500
N1—C5	1.338 (7)	C4—C5	1.380 (8)
N1—C1	1.345 (7)	C5—H5	0.9500
N2—C3	1.361 (7)	C1—H1	0.9500
N2—C6	1.454 (8)	C6—H6a	0.9800
N2—C7	1.457 (7)	C6—H6b	0.9800
C9—C10	1.400 (7)	C6—H6c	0.9800
C9—C8	1.393 (7)	C7—H7a	0.9800
C10—C8^{i}	1.404 (7)	C7—H7b	0.9800
C3—C2	1.411 (8)	C7—H7c	0.9800
C3—C4	1.410 (7)		
C1—N1—C5	116.3 (5)	C5—C4—C3	119.4 (5)

C6—N2—C3	120.3 (5)	C5—C4—H4	120.3 (3)
C7—N2—C3	119.5 (5)	C4—C5—N1	124.6 (5)
C7—N2—C6	119.4 (5)	H5—C5—N1	117.7 (3)
C10—C9—Br1	118.8 (4)	H5—C5—C4	117.7 (3)
C8—C9—Br1	119.3 (4)	C2—C1—N1	123.7 (5)
C8—C9—C10	121.9 (5)	H1—C1—N1	118.1 (3)
C9—C10—Br2	119.1 (4)	H1—C1—C2	118.1 (3)
C8^{i}—C10—Br2	120.0 (4)	H6a—C6—N2	109.5
C8^{i}—C10—C9	121.0 (5)	H6b—C6—N2	109.5
C2—C3—N2	121.9 (5)	H6b—C6—H6a	109.5
C4—C3—N2	122.2 (5)	H6c—C6—N2	109.5
C4—C3—C2	115.9 (5)	H6c—C6—H6a	109.5
C9—C8—I1	121.5 (4)	H6c—C6—H6b	109.5
C10^{i}—C8—I1	121.3 (4)	H7a—C7—N2	109.5
C10^{i}—C8—C9	117.1 (5)	H7b—C7—N2	109.5
H2—C2—C3	120.0 (3)	H7b—C7—H7a	109.5
C1—C2—C3	120.1 (5)	H7c—C7—N2	109.5
C1—C2—H2	120.0 (3)	H7c—C7—H7a	109.5
H4—C4—C3	120.3 (3)	H7c—C7—H7b	109.5

I1—C8—C9—Br1	0.3 (4)	Br2—C10—C8^{i}—C9^{i}	179.2 (4)
I1—C8—C9—C10	179.1 (4)	N1—C5—C4—C3	−0.9 (7)
I1—C8—C10^{i}—Br2^{i}	0.6 (4)	N1—C1—C2—C3	0.4 (7)
I1—C8—C10^{i}—C9^{i}	−179.1 (4)	N2—C3—C2—C1	179.7 (5)
Br1—C9—C10—Br2	−0.4 (4)	N2—C3—C4—C5	−179.4 (5)
Br1—C9—C10—C8^{i}	179.9 (4)	C9—C10—C8^{i}—C9^{i}	−1.1 (4)
Br1—C9—C8—C10^{i}	−179.9 (4)	C9—C8—C10^{i}—C9^{i}	1.1 (4)
Br2—C10—C9—C8	−179.2 (4)		

Symmetry code: (i) −*x*+2, −*y*+2, −*z*+2.

4-(Dimethylamino)pyridine–1-bromo-4-iodo-2,3,5,6-tetrafluorobenzene (2/1) (2DMAP.IBTFB)

Crystal data

$2C_7H_{10}N_2{\cdot}C_6BrF_4I$
M_r = 599.21
Monoclinic, $P2_1/c$
a = 7.3898 (1) Å
b = 16.2120 (2) Å
c = 9.4236 (1) Å
β = 106.304 (2)°
V = 1083.58 (3) Å^3
Z = 2
$F(000)$ = 584.861
D_x = 1.837 Mg m^{-3}
Cu $K\alpha$ radiation, λ = 1.54184 Å
Cell parameters from 6158 reflections
θ = 2.7–77.2°
μ = 14.21 mm^{-1}
T = 100 K
Irregular, clear colourless
0.12 × 0.08 × 0.05 mm

Data collection

Rigaku XtaLAB Synergy Dualflex diffractometer with a HyPix detector
Radiation source: micro-focus sealed X-ray tube, PhotonJet (Cu) X-ray Source
Mirror monochromator
Detector resolution: 10.0000 pixels mm^{-1}
ω scans
Absorption correction: analytical (CrysAlis PRO; Rigaku OD, 2023)
T_{min} = 0.357, T_{max} = 0.595
10454 measured reflections
2300 independent reflections

2252 reflections with $I \geq 2u(I)$
$R_{int} = 0.042$
$\theta_{max} = 77.8°$, $\theta_{min} = 5.5°$

$h = -9 \rightarrow 8$
$k = -20 \rightarrow 20$
$l = -11 \rightarrow 11$

Refinement

Refinement on F^2
Least-squares matrix: full
$R[F^2 > 2\sigma(F^2)] = 0.034$
$wR(F^2) = 0.080$
$S = 1.00$
2300 reflections
142 parameters
2 restraints
17 constraints
Primary atom site location: dual

H-atom parameters constrained
$w = 1/[\sigma^2(F_o^2) + (0.P)^2 + 7.3962P]$
where $P = (F_o^2 + 2F_c^2)/3$
$(\Delta/\sigma)_{max} = -0.0003$
$\Delta\rho_{max} = 0.75$ e Å^{-3}
$\Delta\rho_{min} = -0.58$ e Å^{-3}
Extinction correction: SHELXL, $Fc^* = kFc[1+0.001xFc^2\lambda^3/\sin(2\theta)]^{-1/4}$
Extinction coefficient: 0.00052 (12)

Fractional atomic coordinates and isotropic or equivalent isotropic displacement parameters (Å²)

	x	*y*	*z*	U_{iso}*/U_{eq}	Occ. (<1)
Br1	0.5971 (11)	0.1994 (3)	0.5192 (9)	0.0152 (3)	0.500000
F1	0.8516 (3)	0.05177 (14)	0.5086 (3)	0.0208 (5)	
F2	0.7755 (3)	−0.10968 (14)	0.4932 (3)	0.0225 (5)	
N2	0.8291 (5)	0.6174 (2)	0.5179 (4)	0.0232 (7)	
N1	0.6838 (5)	0.3679 (2)	0.5376 (4)	0.0223 (7)	
C9	0.6759 (5)	0.0271 (2)	0.5040 (4)	0.0166 (7)	
C8	0.5400 (5)	0.0856 (2)	0.5067 (4)	0.0165 (7)	
C3	0.7814 (5)	0.5370 (2)	0.5251 (4)	0.0182 (7)	
C4	0.8329 (5)	0.4914 (2)	0.6585 (4)	0.0196 (8)	
H4	0.9035 (5)	0.5168 (2)	0.7478 (4)	0.0236 (9)*	
C10	0.6374 (5)	−0.0562 (2)	0.4966 (4)	0.0171 (7)	
C1	0.6320 (6)	0.4122 (3)	0.4111 (4)	0.0220 (8)	
H1	0.5583 (6)	0.3852 (3)	0.3247 (4)	0.0264 (10)*	
C5	0.7796 (6)	0.4098 (3)	0.6572 (5)	0.0215 (8)	
H5	0.8137 (6)	0.3811 (3)	0.7488 (5)	0.0258 (10)*	
C2	0.6781 (6)	0.4934 (2)	0.3983 (4)	0.0200 (8)	
H2	0.6407 (6)	0.5202 (2)	0.3049 (4)	0.0241 (9)*	
C6	0.7750 (6)	0.6616 (3)	0.3788 (5)	0.0255 (9)	
H6a	0.826 (4)	0.6332 (11)	0.3067 (12)	0.0383 (13)*	
H6b	0.6371 (6)	0.6635 (18)	0.3418 (19)	0.0383 (13)*	
H6c	0.825 (4)	0.7179 (7)	0.3937 (9)	0.0383 (13)*	
C7	0.9279 (7)	0.6620 (3)	0.6521 (5)	0.0289 (9)	
H7a	0.853 (2)	0.6603 (19)	0.7228 (16)	0.0433 (14)*	
H7b	1.051 (2)	0.6362 (13)	0.696 (2)	0.0433 (14)*	
H7c	0.946 (4)	0.7195 (6)	0.6272 (8)	0.0433 (14)*	
I1	0.6049 (7)	0.21223 (17)	0.5197 (5)	0.0152 (3)	0.500000

Atomic displacement parameters (Å²)

	U^{11}	U^{22}	U^{33}	U^{12}	U^{13}	U^{23}
Br1	0.0184 (4)	0.0075 (9)	0.01871 (18)	−0.0009 (7)	0.0037 (2)	−0.0006 (7)

F1	0.0143 (10)	0.0228 (12)	0.0258 (12)	−0.0028 (9)	0.0063 (9)	−0.0008 (9)
F2	0.0177 (11)	0.0188 (11)	0.0314 (13)	0.0042 (9)	0.0077 (9)	−0.0014 (9)
N2	0.0305 (18)	0.0171 (16)	0.0202 (17)	−0.0049 (14)	0.0042 (14)	0.0000 (13)
N1	0.0174 (15)	0.0232 (18)	0.0257 (18)	0.0008 (13)	0.0051 (13)	0.0012 (14)
C9	0.0152 (16)	0.0190 (19)	0.0140 (17)	−0.0041 (14)	0.0015 (13)	0.0014 (14)
C8	0.0175 (17)	0.0146 (17)	0.0170 (18)	−0.0014 (14)	0.0042 (14)	−0.0003 (14)
C3	0.0187 (17)	0.0188 (18)	0.0191 (18)	−0.0002 (15)	0.0086 (15)	−0.0031 (15)
C4	0.0200 (18)	0.0194 (19)	0.0197 (19)	0.0003 (15)	0.0058 (15)	−0.0010 (15)
C10	0.0177 (17)	0.0175 (18)	0.0167 (18)	0.0023 (14)	0.0057 (14)	0.0005 (14)
C1	0.0222 (19)	0.026 (2)	0.0180 (19)	0.0003 (16)	0.0055 (15)	−0.0035 (16)
C5	0.0233 (19)	0.022 (2)	0.0194 (19)	0.0020 (16)	0.0062 (15)	0.0009 (15)
C2	0.0239 (19)	0.0200 (19)	0.0154 (18)	−0.0003 (15)	0.0041 (15)	0.0006 (15)
C6	0.033 (2)	0.019 (2)	0.025 (2)	0.0001 (17)	0.0101 (18)	0.0021 (16)
C7	0.036 (2)	0.020 (2)	0.027 (2)	−0.0085 (18)	0.0041 (19)	−0.0047 (17)
I1	0.0184 (4)	0.0075 (9)	0.01871 (18)	−0.0009 (7)	0.0037 (2)	−0.0006 (7)

Geometric parameters (Å, º)

Br1—C8	1.888 (6)	C3—C2	1.413 (5)
Br1—I1	0.216 (8)	C4—H4	0.9500
F1—C9	1.348 (4)	C4—C5	1.380 (6)
F2—C10	1.346 (4)	C1—H1	0.9500
N2—C3	1.358 (5)	C1—C2	1.373 (6)
N2—C6	1.448 (5)	C5—H5	0.9500
N2—C7	1.462 (5)	C2—H2	0.9500
N1—C1	1.352 (5)	C6—H6a	0.9800
N1—C5	1.336 (5)	C6—H6b	0.9800
C9—C8	1.388 (5)	C6—H6c	0.9800
C9—C10	1.377 (5)	C7—H7a	0.9800
C8—C10^{i}	1.387 (5)	C7—H7b	0.9800
C8—I1	2.103 (5)	C7—H7c	0.9800
C3—C4	1.415 (6)		
C6—N2—C3	120.7 (3)	H1—C1—N1	117.6 (2)
C7—N2—C3	120.4 (3)	C2—C1—N1	124.8 (4)
C7—N2—C6	118.8 (3)	C2—C1—H1	117.6 (2)
C5—N1—C1	115.2 (4)	C4—C5—N1	125.2 (4)
C8—C9—F1	119.4 (3)	H5—C5—N1	117.4 (2)
C10—C9—F1	118.4 (3)	H5—C5—C4	117.4 (2)
C10—C9—C8	122.1 (3)	C1—C2—C3	119.5 (4)
C9—C8—Br1	121.3 (4)	H2—C2—C3	120.2 (2)
C10^{i}—C8—Br1	122.1 (4)	H2—C2—C1	120.2 (2)
C10^{i}—C8—C9	116.6 (3)	H6a—C6—N2	109.5
I1—C8—C9	121.0 (3)	H6b—C6—N2	109.5
I1—C8—C10^{i}	122.4 (3)	H6b—C6—H6a	109.5
C4—C3—N2	122.4 (4)	H6c—C6—N2	109.5
C2—C3—N2	121.6 (4)	H6c—C6—H6a	109.5
C2—C3—C4	115.9 (4)	H6c—C6—H6b	109.5

H4—C4—C3	120.4 (2)	H7a—C7—N2	109.5
C5—C4—C3	119.2 (4)	H7b—C7—N2	109.5
C5—C4—H4	120.4 (2)	H7b—C7—H7a	109.5
C9—C10—F2	119.0 (3)	H7c—C7—N2	109.5
C8^{i}—C10—F2	119.7 (3)	H7c—C7—H7a	109.5
C8^{i}—C10—C9	121.2 (4)	H7c—C7—H7b	109.5
Br1—C8—C9—F1	−0.8 (4)	F2—C10—C8^{i}—C9^{i}	−179.6 (3)
Br1—C8—C9—C10	179.3 (4)	F2—C10—C8^{i}—I1^{i}	−0.8 (4)
Br1—C8—C10^{i}—F2^{i}	1.1 (5)	N2—C3—C4—C5	−179.9 (4)
Br1—C8—C10^{i}—C9^{i}	−179.2 (4)	N2—C3—C2—C1	−179.6 (4)
F1—C9—C8—C10^{i}	−179.3 (3)	N1—C1—C2—C3	−2.4 (5)
F1—C9—C8—I1	−0.5 (4)	N1—C5—C4—C3	1.4 (5)
F1—C9—C10—F2	−0.5 (4)	C9—C8—C10^{i}—C9^{i}	−0.7 (3)
F1—C9—C10—C8^{i}	179.2 (3)	C9—C10—C8^{i}—C9^{i}	0.7 (4)
F2—C10—C9—C8	179.5 (3)	C9—C10—C8^{i}—I1^{i}	179.5 (3)

Symmetry code: (i) −*x*+1, −*y*, −*z*+1.

4-(Dimethylamino)pyridine–1,2-dibromo-4,5-difluoro-3,6-diiodobenzene (2/1) (2DMAP.DIBFB)

Crystal data

$2C_7H_{10}N_2{\cdot}C_6Br_2F_2I_2$
M_r = 768.02
Triclinic, $P\overline{1}$
a = 9.6158 (4) Å
b = 9.7518 (4) Å
c = 14.8423 (7) Å
α = 74.473 (4)°
β = 85.820 (4)°
γ = 61.476 (4)°
V = 1175.73 (10) Å^3

Z = 2
F(000) = 723.788
D_x = 2.169 Mg m^{-3}
Cu $K\alpha$ radiation, λ = 1.54184 Å
Cell parameters from 12656 reflections
θ = 3.1–77.0°
μ = 25.26 mm^{-1}
T = 100 K
Plate, clear colourless
0.23 × 0.1 × 0.04 mm

Data collection

Rigaku XtaLAB Synergy Dualflex diffractometer with a HyPix detector
Radiation source: micro-focus sealed X-ray tube, PhotonJet (Cu) X-ray Source
Mirror monochromator
Detector resolution: 10.0000 pixels mm^{-1}
ω scans
Absorption correction: analytical (CrysAlis PRO; Rigaku OD, 2023)

T_{min} = 0.055, T_{max} = 0.441
22021 measured reflections
4962 independent reflections
4694 reflections with $I \geq 2u(I)$
R_{int} = 0.063
θ_{max} = 78.5°, θ_{min} = 3.1°
h = −11→12
k = −12→12
l = −18→18

Refinement

Refinement on F^2
Least-squares matrix: full
$R[F^2 > 2\sigma(F^2)]$ = 0.049
$wR(F^2)$ = 0.142
S = 1.03
4962 reflections
275 parameters
0 restraints

32 constraints
Primary atom site location: dual
H-atom parameters constrained
$w = 1/[\sigma^2(F_o^2) + (0.1145P)^2 + 0.3489P]$ where $P = (F_o^2 + 2F_c^2)/3$
$(\Delta/\sigma)_{max}$ = −0.0004
$\Delta\rho_{max}$ = 3.00 e Å^{-3}
$\Delta\rho_{min}$ = −1.94 e Å^{-3}

Fractional atomic coordinates and isotropic or equivalent isotropic displacement parameters (Å²)

	x	*y*	*z*	U_{iso}*/U_{eq}
I1	0.40062 (3)	0.97911 (4)	0.70655 (2)	0.02939 (14)
I2	0.79056 (4)	0.12383 (4)	0.81263 (2)	0.03182 (14)
Br2	0.54649 (6)	0.76869 (6)	0.53272 (3)	0.02882 (15)
Br1	0.72000 (6)	0.37330 (6)	0.58100 (4)	0.03075 (16)
F1	0.4850 (4)	0.6969 (4)	0.8923 (2)	0.0365 (7)
F2	0.6273 (4)	0.3785 (4)	0.9317 (2)	0.0396 (7)
N1	0.2482 (6)	1.3018 (6)	0.6717 (4)	0.0349 (10)
N2	0.0075 (6)	1.8081 (7)	0.6108 (4)	0.0360 (10)
N3	0.9490 (6)	−0.2038 (6)	0.8602 (4)	0.0376 (10)
N4	1.1802 (6)	−0.7074 (7)	0.9133 (4)	0.0392 (11)
C12	0.6494 (5)	0.4759 (6)	0.6795 (3)	0.0257 (9)
C8	0.5171 (6)	0.7235 (6)	0.7292 (4)	0.0262 (9)
C1	0.2447 (6)	1.5495 (7)	0.6697 (4)	0.0290 (10)
C5	0.0864 (6)	1.6428 (7)	0.6311 (3)	0.0272 (9)
C13	0.5739 (5)	0.6440 (6)	0.6585 (3)	0.0251 (9)
C11	0.6720 (6)	0.3808 (6)	0.7722 (4)	0.0267 (10)
C3	0.0972 (6)	1.3892 (7)	0.6354 (4)	0.0336 (11)
C9	0.5373 (6)	0.6278 (7)	0.8202 (4)	0.0311 (10)
C4	0.0143 (6)	1.5545 (7)	0.6148 (4)	0.0313 (10)
C2	0.3179 (6)	1.3846 (7)	0.6872 (4)	0.0334 (11)
C10	0.6122 (6)	0.4623 (7)	0.8411 (4)	0.0321 (10)
C17	0.9472 (6)	−0.4472 (7)	0.8581 (4)	0.0347 (11)
C16	0.8784 (7)	−0.2829 (8)	0.8424 (4)	0.0380 (12)
C15	1.1001 (7)	−0.2938 (7)	0.8956 (4)	0.0352 (11)
C18	1.1063 (6)	−0.5444 (7)	0.8958 (4)	0.0304 (10)
C14	1.1818 (6)	−0.4598 (7)	0.9140 (4)	0.0333 (11)
C6	−0.1606 (6)	1.8945 (7)	0.5886 (5)	0.0383 (12)
C7	0.0866 (6)	1.8924 (7)	0.6323 (4)	0.0352 (11)
C19	1.0981 (8)	−0.7907 (8)	0.8951 (5)	0.0424 (13)
C20	1.3464 (8)	−0.8058 (8)	0.9470 (6)	0.0496 (16)
H1	0.2999 (6)	1.6011 (7)	0.6834 (4)	0.0348 (12)*
H4	−0.0923 (6)	1.6100 (7)	0.5894 (4)	0.0376 (12)*
H14	1.2888 (6)	−0.5176 (7)	0.9388 (4)	0.0400 (13)*
H17	0.8890 (6)	−0.4956 (7)	0.8438 (4)	0.0417 (13)*
H6a	−0.1829 (7)	1.887 (6)	0.5273 (18)	0.0575 (18)*
H6b	−0.2125 (9)	1.847 (4)	0.637 (2)	0.0575 (18)*
H6c	−0.2011 (12)	2.0085 (15)	0.587 (4)	0.0575 (18)*
H7a	0.101 (6)	1.869 (5)	0.7005 (4)	0.0529 (17)*
H7b	0.190 (3)	1.856 (5)	0.605 (3)	0.0529 (17)*
H7c	0.021 (3)	2.0093 (8)	0.606 (3)	0.0529 (17)*
H19a	1.002 (4)	−0.763 (6)	0.930 (3)	0.0636 (19)*
H19b	1.069 (6)	−0.758 (5)	0.8279 (7)	0.0636 (19)*
H19c	1.168 (3)	−0.9079 (8)	0.915 (4)	0.0636 (19)*
H20a	1.4084 (14)	−0.757 (4)	0.910 (3)	0.074 (2)*
H20b	1.3569 (12)	−0.811 (7)	1.0132 (14)	0.074 (2)*

H20c	1.386 (2)	−0.915 (2)	0.940 (4)	0.074 (2)*
H3	0.0454 (6)	1.3331 (7)	0.6235 (4)	0.0403 (13)*
H2	0.4250 (6)	1.3250 (7)	0.7119 (4)	0.0400 (13)*
H15	1.1535 (7)	−0.2400 (7)	0.9087 (4)	0.0422 (13)*
H16	0.7718 (7)	−0.2206 (8)	0.8168 (4)	0.0456 (14)*

Atomic displacement parameters (Å²)

	U^{11}	U^{22}	U^{33}	U^{12}	U^{13}	U^{23}
I1	0.0264 (2)	0.0275 (2)	0.0354 (2)	−0.01116 (15)	−0.00138 (12)	−0.01253 (14)
I2	0.0300 (2)	0.0277 (2)	0.0357 (2)	−0.01197 (16)	−0.00371 (13)	−0.00713 (14)
Br2	0.0297 (3)	0.0295 (3)	0.0269 (3)	−0.0135 (2)	−0.00174 (18)	−0.0074 (2)
Br1	0.0323 (3)	0.0306 (3)	0.0308 (3)	−0.0132 (2)	0.00128 (19)	−0.0139 (2)
F1	0.0482 (17)	0.0334 (16)	0.0300 (14)	−0.0177 (14)	0.0055 (12)	−0.0162 (12)
F2	0.0489 (17)	0.0399 (18)	0.0280 (14)	−0.0198 (15)	0.0013 (12)	−0.0080 (13)
N1	0.033 (2)	0.034 (3)	0.038 (2)	−0.013 (2)	−0.0033 (18)	−0.013 (2)
N2	0.028 (2)	0.037 (3)	0.044 (3)	−0.013 (2)	−0.0039 (18)	−0.017 (2)
N3	0.038 (2)	0.030 (2)	0.042 (3)	−0.015 (2)	−0.0056 (19)	−0.0049 (19)
N4	0.035 (2)	0.034 (3)	0.043 (3)	−0.011 (2)	−0.009 (2)	−0.010 (2)
C12	0.024 (2)	0.026 (2)	0.032 (2)	−0.0121 (18)	0.0011 (16)	−0.0142 (19)
C8	0.0194 (19)	0.026 (2)	0.033 (2)	−0.0094 (19)	−0.0002 (16)	−0.0105 (19)
C1	0.028 (2)	0.035 (3)	0.031 (2)	−0.019 (2)	0.0023 (18)	−0.013 (2)
C5	0.024 (2)	0.028 (2)	0.027 (2)	−0.0095 (19)	0.0007 (16)	−0.0100 (19)
C13	0.027 (2)	0.027 (2)	0.0214 (19)	−0.0140 (19)	−0.0010 (15)	−0.0037 (17)
C11	0.026 (2)	0.021 (2)	0.034 (2)	−0.0109 (19)	0.0000 (18)	−0.0077 (19)
C3	0.029 (2)	0.038 (3)	0.039 (3)	−0.017 (2)	−0.0026 (19)	−0.016 (2)
C9	0.030 (2)	0.037 (3)	0.032 (2)	−0.015 (2)	0.0013 (18)	−0.019 (2)
C4	0.024 (2)	0.034 (3)	0.037 (2)	−0.013 (2)	−0.0007 (18)	−0.012 (2)
C2	0.025 (2)	0.036 (3)	0.040 (3)	−0.013 (2)	−0.0026 (19)	−0.014 (2)
C10	0.034 (2)	0.039 (3)	0.026 (2)	−0.020 (2)	−0.0008 (18)	−0.006 (2)
C17	0.030 (2)	0.037 (3)	0.037 (3)	−0.016 (2)	0.000 (2)	−0.008 (2)
C16	0.032 (2)	0.039 (3)	0.037 (3)	−0.013 (2)	−0.005 (2)	−0.006 (2)
C15	0.038 (3)	0.034 (3)	0.035 (2)	−0.018 (2)	−0.001 (2)	−0.009 (2)
C18	0.030 (2)	0.031 (3)	0.026 (2)	−0.010 (2)	−0.0016 (18)	−0.009 (2)
C14	0.029 (2)	0.034 (3)	0.035 (2)	−0.013 (2)	−0.0021 (19)	−0.010 (2)
C6	0.027 (2)	0.030 (3)	0.051 (3)	−0.007 (2)	−0.003 (2)	−0.012 (2)
C7	0.031 (2)	0.030 (3)	0.048 (3)	−0.013 (2)	0.002 (2)	−0.017 (2)
C19	0.043 (3)	0.037 (3)	0.048 (3)	−0.017 (3)	0.002 (2)	−0.016 (3)
C20	0.037 (3)	0.031 (3)	0.069 (4)	−0.002 (2)	−0.009 (3)	−0.016 (3)

Geometric parameters (Å, º)

I1—C8	2.127 (5)	C3—C4	1.368 (8)
I2—C11	2.123 (5)	C3—H3	0.9500
Br2—C13	1.894 (5)	C9—C10	1.369 (8)
Br1—C12	1.894 (5)	C4—H4	0.9500
F1—C9	1.354 (6)	C2—H2	0.9500
F2—C10	1.351 (6)	C17—C16	1.367 (9)

N1—C3	1.346 (7)	C17—C18	1.417 (7)
N1—C2	1.338 (8)	C17—H17	0.9500
N2—C5	1.368 (8)	C16—H16	0.9500
N2—C6	1.435 (7)	C15—C14	1.375 (8)
N2—C7	1.459 (8)	C15—H15	0.9500
N3—C16	1.327 (8)	C18—C14	1.414 (8)
N3—C15	1.343 (8)	C14—H14	0.9500
N4—C18	1.352 (8)	C6—H6a	0.9800
N4—C19	1.455 (8)	C6—H6b	0.9800
N4—C20	1.456 (8)	C6—H6c	0.9800
C12—C13	1.391 (7)	C7—H7a	0.9800
C12—C11	1.403 (7)	C7—H7b	0.9800
C8—C13	1.394 (7)	C7—H7c	0.9800
C8—C9	1.388 (8)	C19—H19a	0.9800
C1—C5	1.414 (7)	C19—H19b	0.9800
C1—C2	1.368 (8)	C19—H19c	0.9800
C1—H1	0.9500	C20—H20a	0.9800
C5—C4	1.409 (8)	C20—H20b	0.9800
C11—C10	1.385 (8)	C20—H20c	0.9800

C2—N1—C3	116.7 (5)	C9—C10—C11	121.8 (5)
C6—N2—C5	119.9 (5)	C18—C17—C16	119.2 (5)
C7—N2—C5	119.3 (5)	H17—C17—C16	120.4 (3)
C7—N2—C6	119.3 (5)	H17—C17—C18	120.4 (3)
C15—N3—C16	116.6 (5)	C17—C16—N3	125.1 (5)
C19—N4—C18	121.0 (5)	H16—C16—N3	117.5 (3)
C20—N4—C18	121.5 (5)	H16—C16—C17	117.5 (3)
C20—N4—C19	117.4 (5)	C14—C15—N3	123.5 (5)
C13—C12—Br1	119.5 (4)	H15—C15—N3	118.2 (3)
C11—C12—Br1	119.3 (4)	H15—C15—C14	118.2 (3)
C11—C12—C13	121.2 (5)	C17—C18—N4	121.8 (5)
C13—C8—I1	124.6 (4)	C14—C18—N4	122.5 (5)
C9—C8—I1	118.2 (4)	C14—C18—C17	115.7 (5)
C9—C8—C13	117.1 (5)	C18—C14—C15	119.9 (5)
C2—C1—C5	119.7 (5)	H14—C14—C15	120.0 (3)
H1—C1—C5	120.2 (3)	H14—C14—C18	120.0 (3)
H1—C1—C2	120.2 (3)	H6a—C6—N2	109.5
C1—C5—N2	122.4 (5)	H6b—C6—N2	109.5
C4—C5—N2	121.9 (5)	H6b—C6—H6a	109.5
C4—C5—C1	115.7 (5)	H6c—C6—N2	109.5
C12—C13—Br2	120.1 (4)	H6c—C6—H6a	109.5
C8—C13—Br2	118.9 (4)	H6c—C6—H6b	109.5
C8—C13—C12	120.9 (4)	H7a—C7—N2	109.5
C12—C11—I2	124.4 (4)	H7b—C7—N2	109.5
C10—C11—I2	118.7 (4)	H7b—C7—H7a	109.5
C10—C11—C12	116.9 (5)	H7c—C7—N2	109.5
C4—C3—N1	123.5 (5)	H7c—C7—H7a	109.5
H3—C3—N1	118.3 (3)	H7c—C7—H7b	109.5

H3—C3—C4	118.3 (3)	H19a—C19—N4	109.5
C8—C9—F1	120.3 (5)	H19b—C19—N4	109.5
C10—C9—F1	117.7 (5)	H19b—C19—H19a	109.5
C10—C9—C8	122.0 (5)	H19c—C19—N4	109.5
C3—C4—C5	120.2 (5)	H19c—C19—H19a	109.5
H4—C4—C5	119.9 (3)	H19c—C19—H19b	109.5
H4—C4—C3	119.9 (3)	H20a—C20—N4	109.5
C1—C2—N1	124.2 (5)	H20b—C20—N4	109.5
H2—C2—N1	117.9 (3)	H20b—C20—H20a	109.5
H2—C2—C1	117.9 (3)	H20c—C20—N4	109.5
C11—C10—F2	120.1 (5)	H20c—C20—H20a	109.5
C9—C10—F2	118.1 (5)	H20c—C20—H20b	109.5
I1—C8—C13—Br2	−0.3 (4)	F2—C10—C11—C12	178.9 (5)
I1—C8—C13—C12	179.7 (4)	F2—C10—C9—C8	179.7 (4)
I1—C8—C9—F1	−0.7 (4)	N1—C3—C4—C5	0.2 (7)
I1—C8—C9—C10	−179.4 (4)	N1—C2—C1—C5	−1.3 (7)
I2—C11—C12—Br1	2.7 (4)	N2—C5—C1—C2	−179.1 (5)
I2—C11—C12—C13	−178.4 (4)	N2—C5—C4—C3	179.6 (5)
I2—C11—C10—F2	−1.2 (4)	N3—C16—C17—C18	−0.3 (7)
I2—C11—C10—C9	178.7 (4)	N3—C15—C14—C18	−0.2 (7)
Br2—C13—C12—Br1	−1.5 (4)	N4—C18—C17—C16	179.6 (6)
Br2—C13—C12—C11	179.6 (4)	N4—C18—C14—C15	−179.3 (6)
Br2—C13—C8—C9	179.0 (4)	C12—C13—C8—C9	−1.0 (5)
Br1—C12—C13—C8	178.5 (3)	C12—C11—C10—C9	−1.3 (6)
Br1—C12—C11—C10	−177.4 (4)	C8—C9—C10—C11	−0.2 (6)
F1—C9—C8—C13	180.0 (5)	C1—C5—C4—C3	−0.5 (6)
F1—C9—C10—F2	1.0 (5)	C17—C18—C14—C15	0.5 (6)
F1—C9—C10—C11	−178.9 (4)		